5.2 Leg M45/2

5.2.1 Hydrography Including Nutrients

(S. Becker, L. Böhme, T. Csernok, H. Dietze, H. Johannsen, T. J. Müller, M. Reich and W. Zenk)

The Data Set

Table 7.2.1 contains summaries of the hydrographic station work. The backbone of the hydrographic observations consisted of 64 CTD profiles (casts). 56 casts included profiles of a lowered Acoustic Doppler Current Profiler (LADCP). 1091 water samples were analyzed already on board in respect to nutrient salts (NO_3, NO_2, PO_4, SiO_4) and dissolved oxygen. In addition to CTD temperature and salinity from bottles, nutrient data represent a valuable set of parameters, (almost) independent of the distribution of temperature and salt. The O_2 data will be used to optimize the calibration of the continuously measuring oxygen sensor integrated in the CTD system (IfM code NB-3). A potential drift of the primary CTD sensor package for electrical **C**onductivity, **T**emperature and Pressure (**D**epth) was monitored by 308 salinity check values plus digital reversing thermometers and pressure readings. These additional sensors were mounted on selected bottles of the rosette sampler.

CTD/Rosette Sampler and Thermosalinograph: Performance and Calibration Checks

A single MKIIIB type CTD instrument was used throughout leg M45/2. Laboratory calibration of the temperature and pressure sensors and *in situ* calibration of the conductivity sensor followed the routines described by MÜLLER (1999). Pre-cruise laboratory calibration for the temperature and pressure sensors are from from March 1999, i.e. from three months before the cruise. From the history of this individual CTD probe it is known that both sensors have small drifts only: < 2 mK/a and < 1 dbar/a, respectively, for the whole range. *In situ* cross checks during the cruise with the reversing eletronic temperature and pressure sensors did not show any jump or drift within their resolution (1 mK and 1 dbar, respectively). Therefore, the errors due to drifts of both these sensors are expected to be negligibly small, and no post-cruise

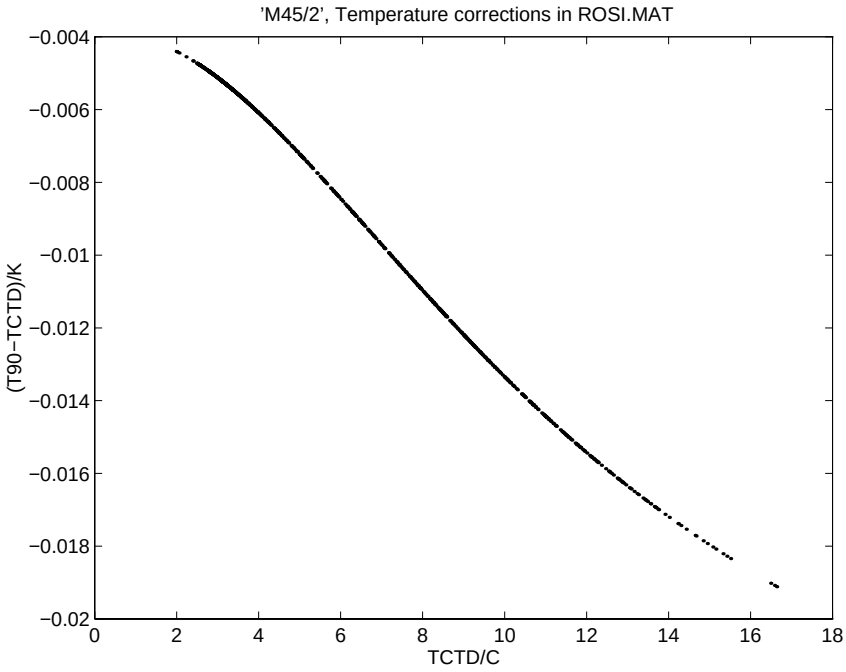

Fig. 21: Corrections (T90-TCTD) applied to the CTD's temperature sensor output TCTD according to the March 1999 laboratory calibration. Shown are values taken while bottles were closed. The expected error is < 2 mK over the whole range.

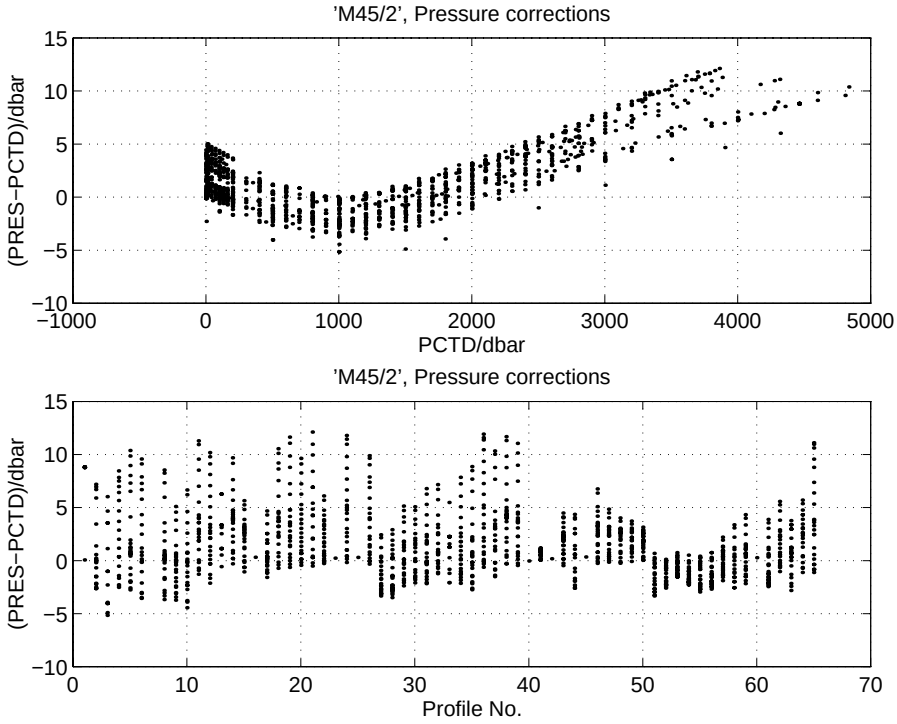

Fig. 22: Corrections (PRES-PCTD) applied to the CTD's pressure sensor output PCTD according to the March 1999 laboratory calibration including corrections due to hysteresis and dynamic temperature effects. Shown are values taken during while bottles were closed. The expected error is < 3 dbar at maximum pressure.

calibration is applied. The expected overall error for the calibrated CTD temperature (Fig. 21) is < 2 mK, the one for pressure (Fig. 22) is < 3 dbar at maximum pressure (6000 dbar).

The conductivity sensor showed drifts and jumps and needed a calibration in 5 batches of profiles (casts). For each batch, *in situ* conductivity was derived from calibrated temperature and pressure and from bottle salinities. A polynomial fit in conductivity, pressure and profile number (drift) was used for correction for each batch (Fig. 23). Prior to calibration, salinity comparisons (and nutrient and oxygen distributions) were used to identify and re-arrange those bottles that did not close at the nominal pressure due to technical problems with the rosette firing system. The overall error estimate in corrected salinity is < 0.004.

The temperature and salinity measurements of the shipborne thermosalinograph (4 m depth) were compared with calibrated CTD values from 10 m depth. Over leg M45/2 the corrections to be applied are -0.05 K with a **r**oot **m**ean **s**quare value of 0.1 K for temperature, and 0.017 (rms = 0.03) for salinity. A slight trend to higher salinity corrections at the end of leg M45/2 seems to be insignificant.

Horizontal Distribution of Temperature and Salinity

The Iceland Basin is influenced by the anticyclonic subtropical and the cyclonic subpolar gyres. The **N**orth **A**tlantic **C**urrent (NAC) which separates these two regimes in the western North Atlantic is fed by the Gulf Stream and substantiates the Subpolar Front in the Iceland Basin. Rossby (1999) identifies the path of the NAC by the 10°C-isotherm in his figure of the mean March sea surface temperature (SST) in the North Atlantic. A comparison of Figure 24a with his surface temperature shows that in the Newfoundland Basin northeast from the Grand Banks the temperature decreases to the east in the same way. We can also see that in the eastern Basin the temperature decreases substantially to the north whereby in the east the warmer waters of subtropical origin penetrate towards Rockall.

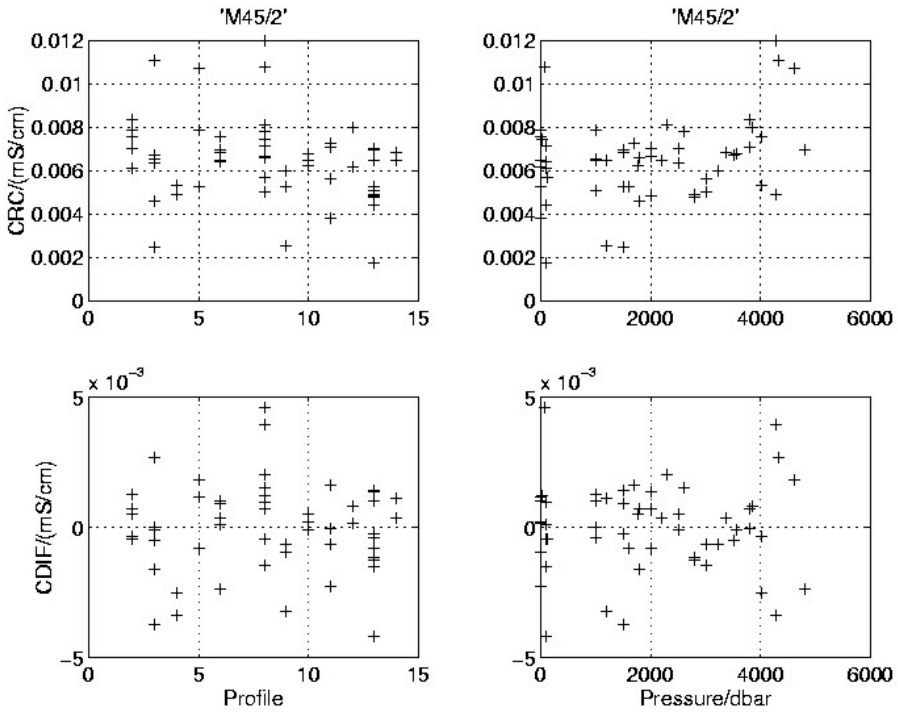

Fig. 23: Corrections are applied to the CTD's conductivity sensor output according to comparisons with in situ conductivity. Shown are derived salinity corrections SRC and residuals SDIF for the batch of profiles (casts) 41 to 60. The expected overall error for all profiles is < 0.004 in salinity.

In Figure 24b the highest values of salinity from subtropical waters were recorded in the southeast. In the west there are lower values due to fresher waters from the subpolar gyre with the exception of some high values northeast from Grand Banks. There the NAC comes from the south and turns to the east, so that fresher and colder water is west- and northward of it.

Vessel mounted Acoustic Doppler Current Profiler (VM-ADCP)

During the cruise the VM-ADCP continuously recorded currents upper layers. Figure 25 shows currents along all sections in 21 - 100 m and 300 - 600 m depth. The currents in 100 - 300 m depth (not displayed here) are very similar to those in 300 - 600 m.

Although the sea surface currents in Figure 25 are superimposed by eddies and tidal currents they support the cyclonic circulation in the Iceland Basin that we expected. Maximum values of 60 cm/s are found in 21 - 100 m depth at section F + G with northeast direction.

Vertical Parameter Distribution: Sections and θ/S Diagrams

In 1997 we had introduced a work nomenclature for eastern basin sections (SCHOTT ET AL., 1999) which we have retained during this cruise. (For location see Fig.4):

Sec.	F+G	connecting the Mid-Atlantic Ridge with the continental slope of Europe
Sec.	E	crossing Charlie Gibbs Fracture Zone (CGFZ)
Sec.	D	connecting southern end of Reykjanes Ridge with CGFZ
Sec.	A	connecting Rockall Bank with Reykjanes Ridge
Sec.	I	northern section off Iceland in preparation for POSEIDON cruise in 2000
Sec.	L	parallel section to Maury Channel, at 2800 m, unfinished due to severe weather conditions

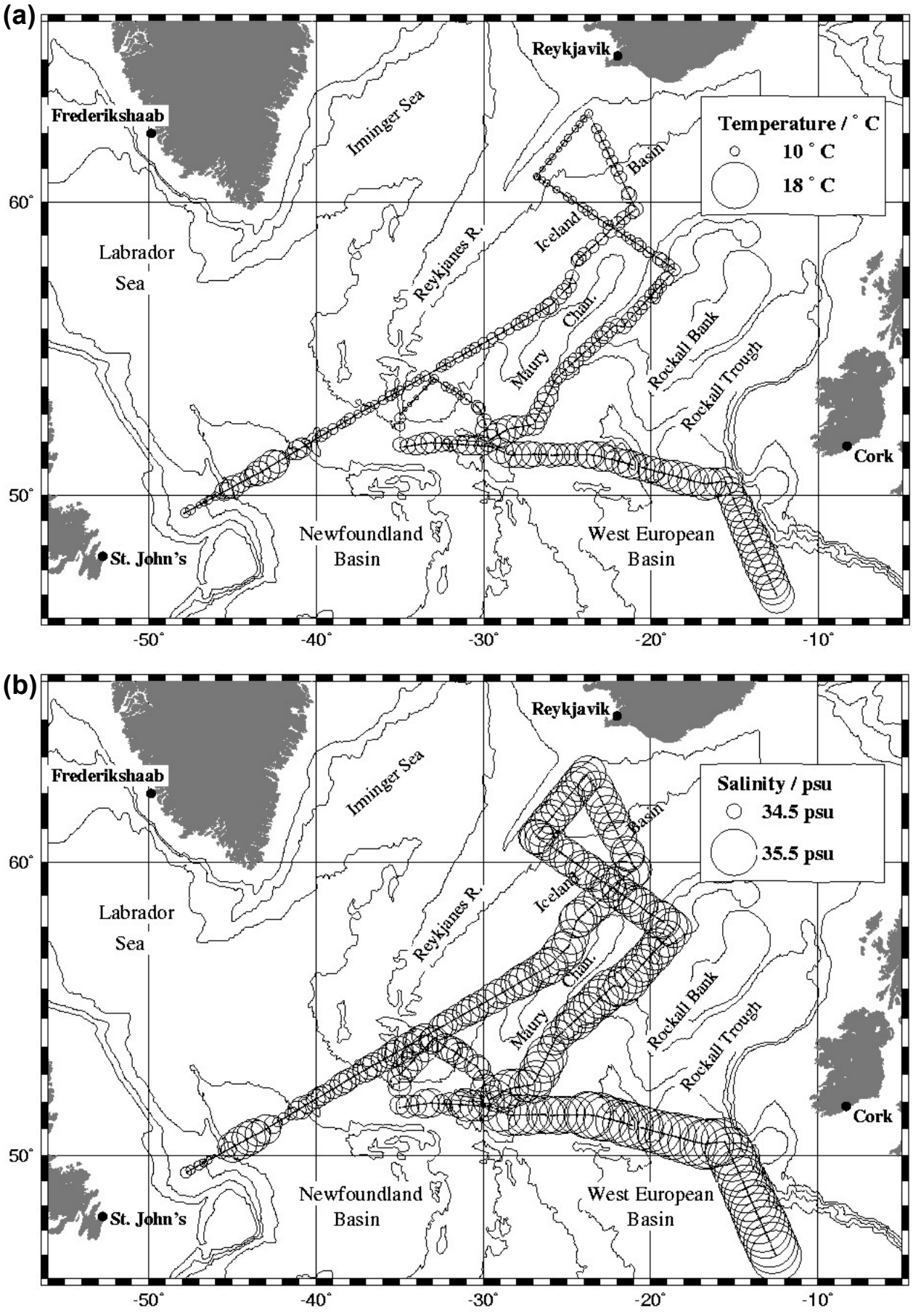

Fig. 24: Distribution of temperature (a) and salinity (b) at the sea surface in June/July 1999 from continuous measurements with the ship's thermosalinograph.

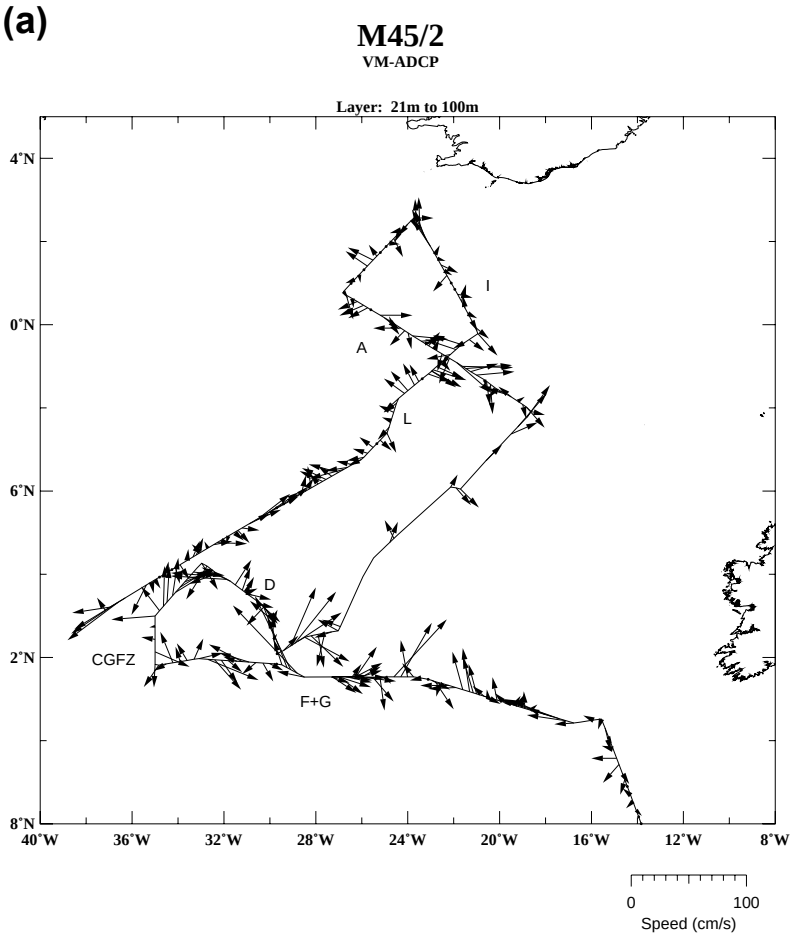

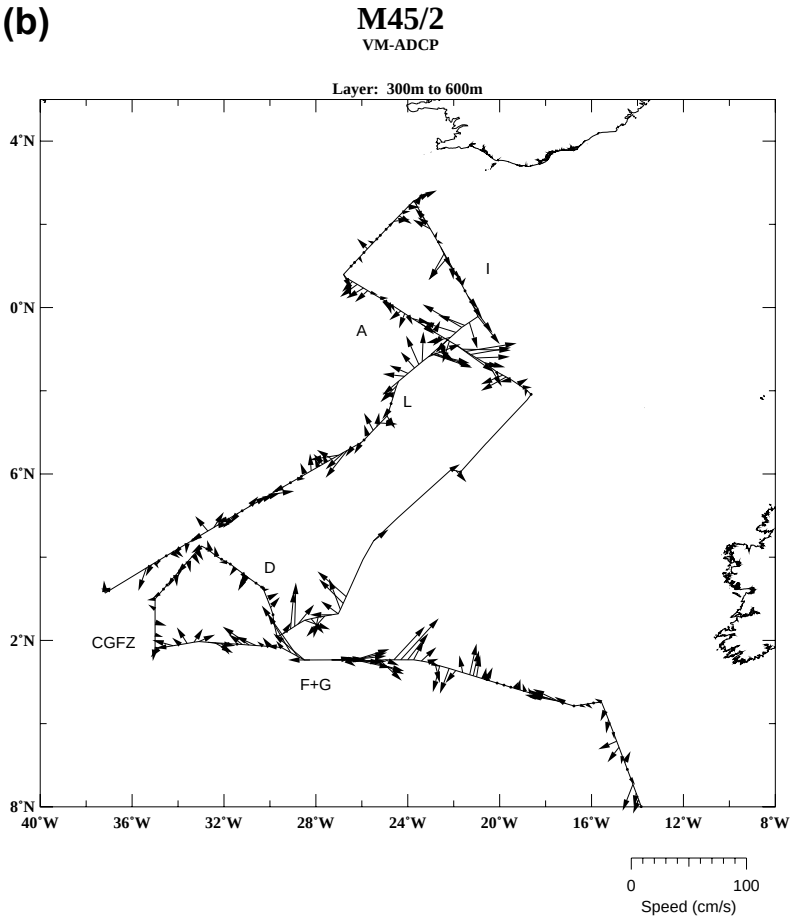

Fig. 25a/b: Currents from measurements with the VM-ADCP (a) in 21 - 100 m depth and (b) in 300 - 600 m depth. Capital letters indicate the sections.

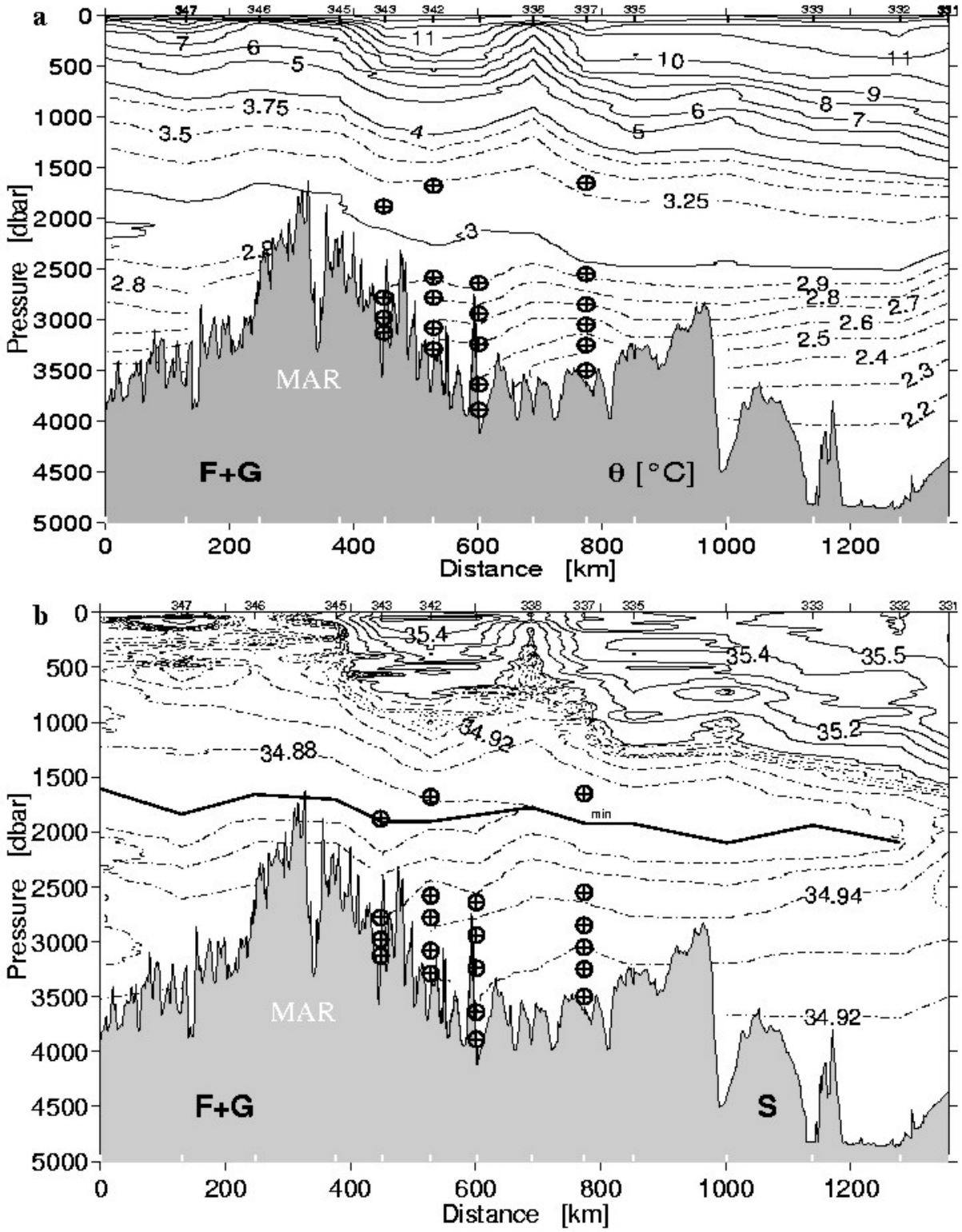

Fig. 26: Distribution of potential temperature (a), salinity (b), oxygen (c), silicate (d), nitrate (e) and phosphate (f) along section F+G. Marks show observation levels of current meters of the recovered array MART (see also 5.2.2). Heavy lines in (b), (c) and (e) label intermediate extrema in context with eastward propagating Labrador Sea Water. Bold station numbers indicate selected stations for θ-S diagram (Fig. 30).

Fig. 26 shows the vertical distributions of potential temperature (θ), salinity (S), oxygen (O_2), silicate (SiO_4), nitrate (NO_3) and phosphate (PO_4) along the southern section F+G. We also show the distribution of salinity, temperature, oxygen and nitrate along sections D (Fig. 27), A (Fig. 28) and I (Fig. 29). For

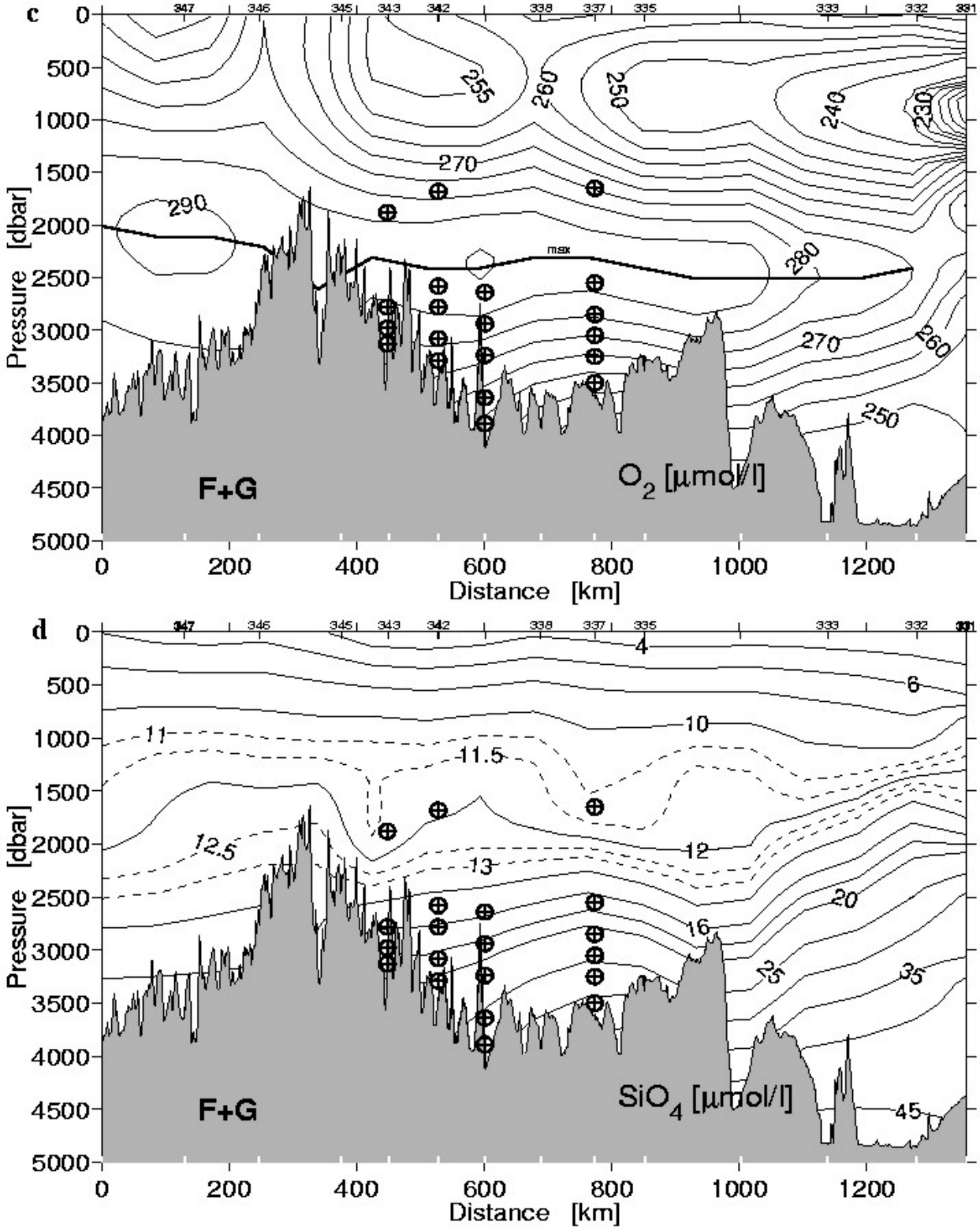

Fig. 26: continued

additional information we have included observation levels of current meters of the recovered array M A R T (Fig. 26) as well as in the newly deployed array C G F Z (Fig. 27) (see also Table 7.2.2). Information on the concurrent surveys with the lowered current profiler (LADCP) is given from Sec. A and I in Fig. 31.

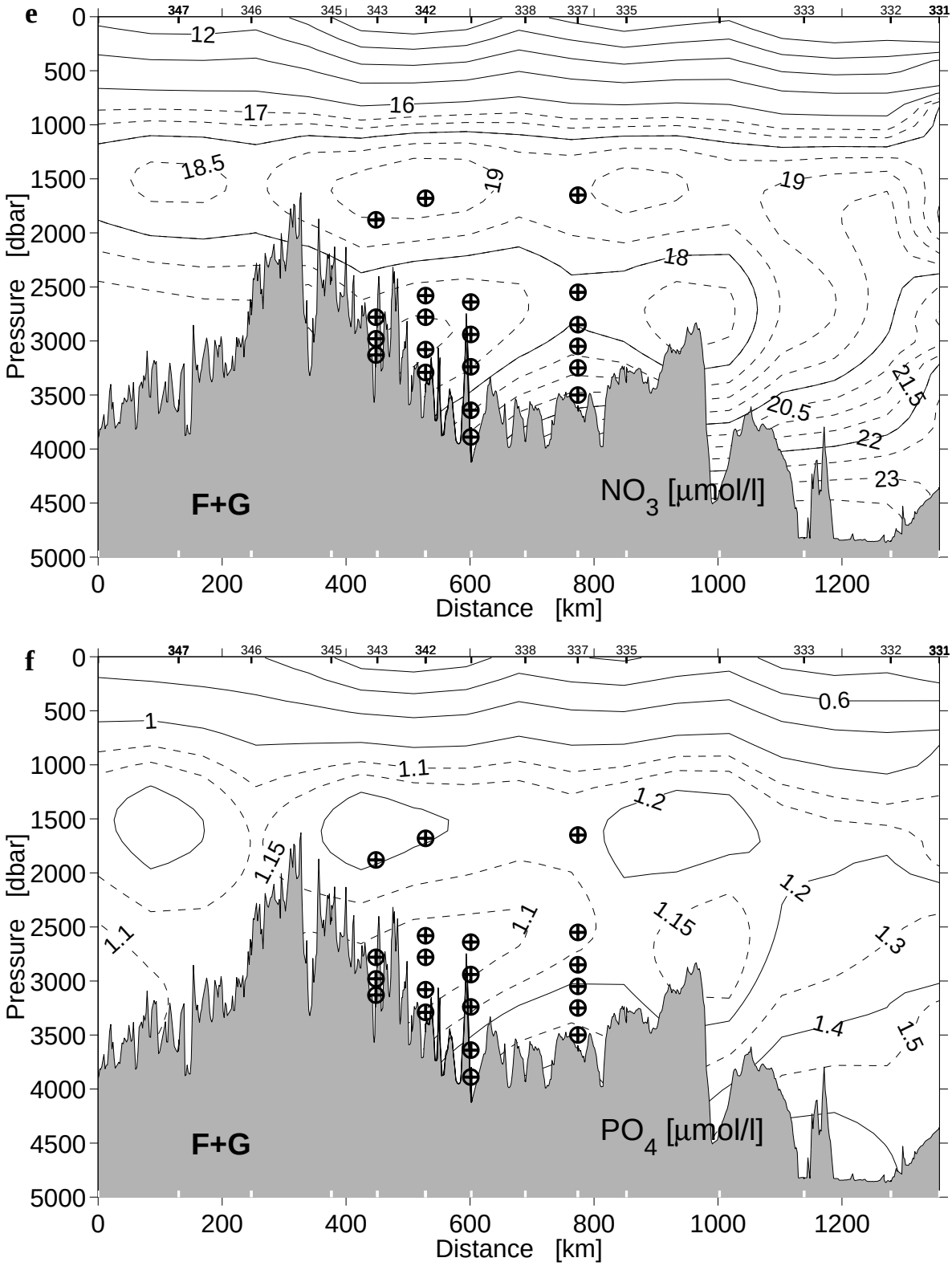

Fig. 26: continued

The water masses in the Iceland Basin which can be identified in the sections are:

- Subpolar Mode Water (SPMW)
- Mediterranean Water (MW)
- Labrador Sea Water (LSW)
- Lower Deep Water (LDW)
- Iceland Scotland Overflow Water (ISOW)

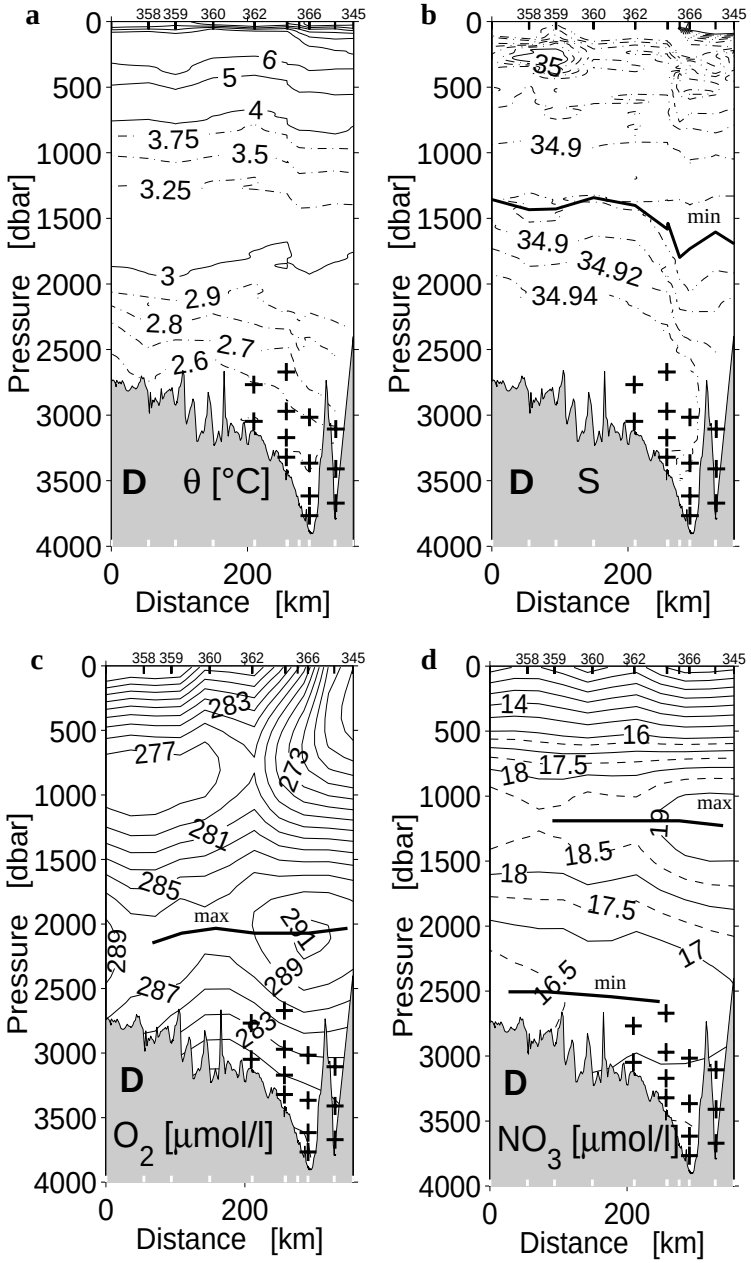

Fig. 27: Distribution of potential temperature (a), salinity (b), oxygen (c) and nitrate (d) along section D. Marks show observation levels of current meters in the newly deployed array CGFZ (cf. Tab. 7.2.2).

SPMW in section F+G shows higher temperature and salinity on the eastern side (Fig. 26 a,b). LSW which is characterized by the low salinity core (S < 34.90) can also be identified by its temperature (3 - 3.5°C), high oxygen (~280 µmol/kg) and moderate values of silicate (~10.5 µmol/kg) in the Iceland Basin (VAN AKEN AND BECKER, 1996). In section F+G we can clearly identify LSW by the low salinity tongue, which enters the basin through CGFZ in about 1500 dbar. LDW has a temperature of about 2°C and a salinity of 34.90 (VAN AKEN AND BECKER, 1996) and can be identified by its oxygen minimum and silicate and nitrate maximum (VAN AKEN AND DE BOER, 1995). In Section F+G we find LDW in the West European Basin in depths > 4000 m with O_2~250 µmol/l, SiO_4~45 µmol/l and NO_3~23 µmol/l. ISOW has a salinity and oxygen maximum and a silicate and nitrate minimum (VAN AKEN AND DE BOER, 1995). For their water mass analysis they chose θ = 1.75 and S = 35.00. The Iceland Basin ISOW has a temperature of about 2.5°C and salinity of 34.98 (VAN AKEN AND BECKER, 1996). It can be identified clearly in section F+G by its oxygen maximum (280 - 290 µmol/l) and nitrate minimum (17 - 18 µmol/l) at a pressure range of 2000 - 3500 dbar.

On section A (Fig. 28) and I (Fig. 29) we see ISOW with an oxygen maximum of 290 µmol/l and a nitrate minimum at the bottom and at the flank of the Reykjanes Ridge. LSW with its salinity minimum can be found in 1500 - 2000 dbar.

Fig. 30 shows a θ-S diagram of six selected stations marked with double circles in Fig. 4 and bold numbers in Fig. 26-29. The surface water (a) is saltiest in the West European Basin (Station 331, see also Fig. 24b). At this station we also have influence from MW with a temperature of 8°C and salinity > 35.4. Other profiles show that between the CGFZ and the northern Iceland Basin salinity increases in the SPMW. In the deep water diagram (b) we can see that the LSW near CGFZ (Station 347, 350) is the coldest and freshest water type. On its way through the Iceland Basin it becomes more saline and warmer due to mixing. LDW with temperature of about 2°C and salinity of 34.90 is found only at station 331 in the West

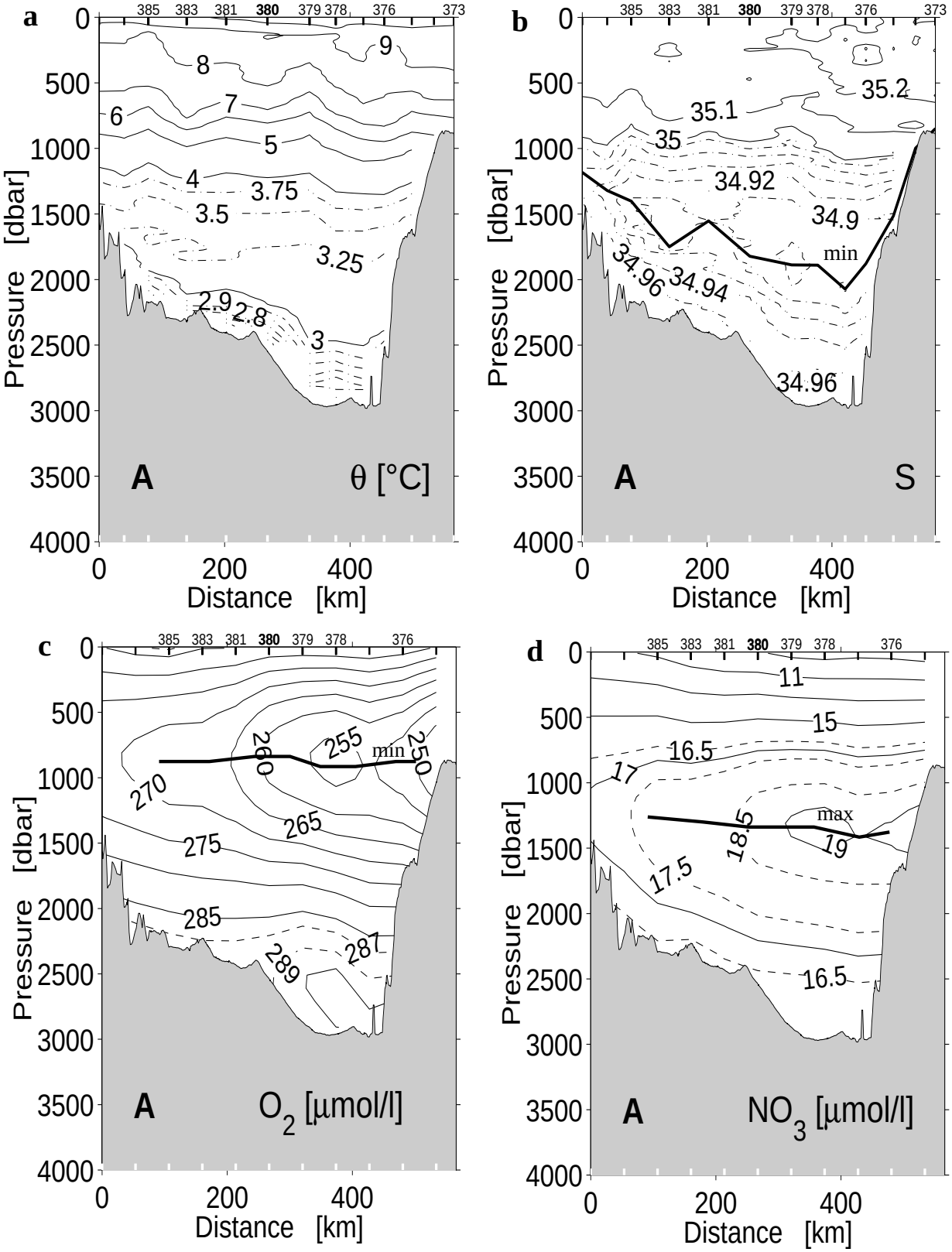

Fig. 28: Distribution of potential temperature (a), salinity (b), oxygen (c) and nitrate (d) along section A. Bold station numbers indicate selected stations for θ-S diagram (Fig. 30).

European Basin and at station 350. The ISOW (θ ~ 2.5, S ~ 34.94) is more saline in the northern Iceland Basin similar to the LSW.

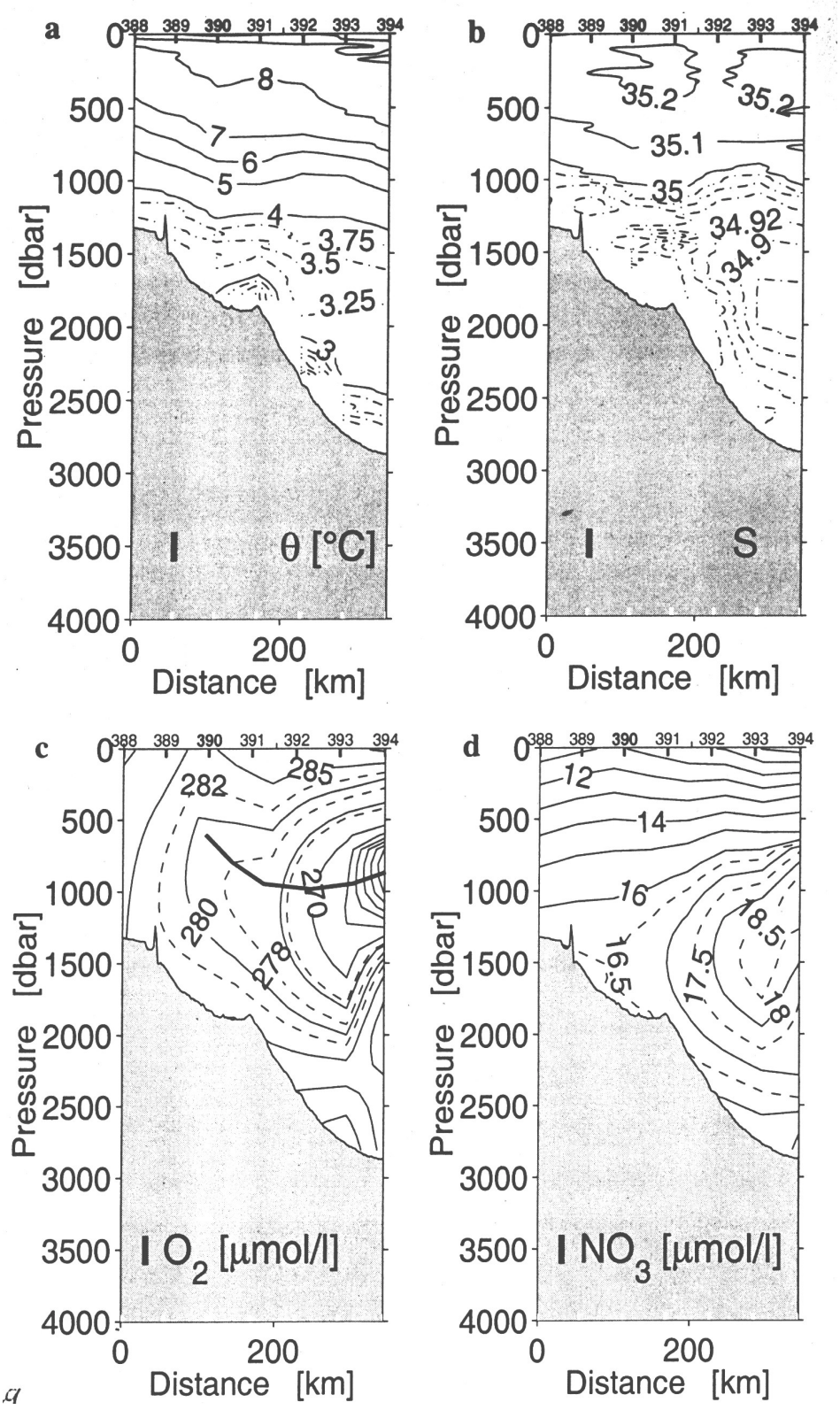

Fig. 29: Distribution of potential temperature (a), salinity (b), oxygen (c) and nitrate (d) along section I. Bold station numbers indicate selected stations for θ-S diagram (Fig. 30).

Lowered Acoustic Doppler Current Profiler (LADCP)

During 56 casts we obtained vertical profiles of horizontal currents. We used a Janus shaped set of two new instruments by RD Instruments of San Diego, CA, one of each looking downward and upward. A third device was kept on board as a backup. Unfortunately, this master/ slave configuration showed transmission problems while communicating with the instruments on board. Additional instrument failures

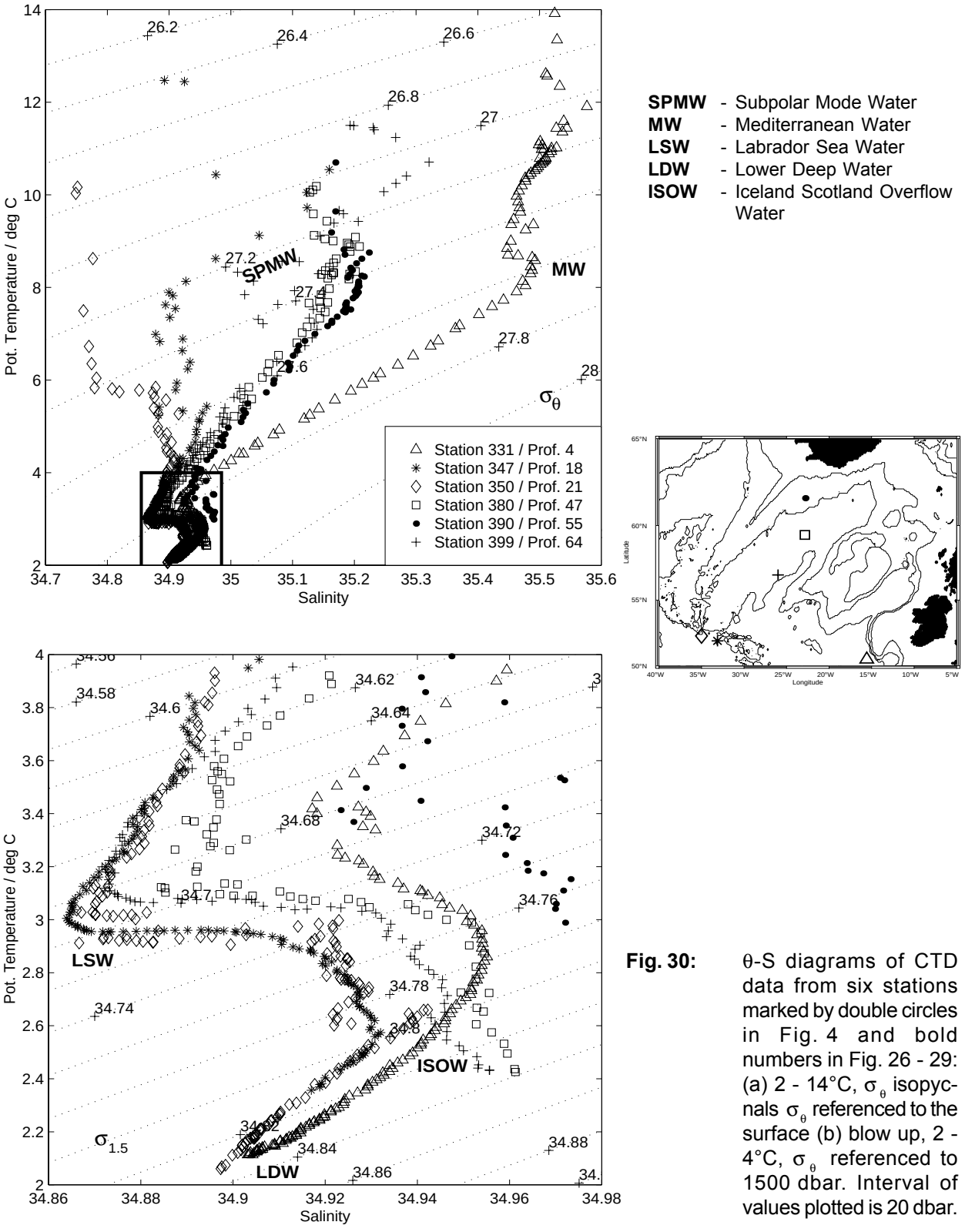

Fig. 30: θ-S diagrams of CTD data from six stations marked by double circles in Fig. 4 and bold numbers in Fig. 26 - 29: (a) 2 - 14°C, σ_θ isopycnals σ_θ referenced to the surface (b) blow up, 2 - 4°C, σ_θ referenced to 1500 dbar. Interval of values plotted is 20 dbar.

occurred at depth. It was decided to use the backup instrument and, as this did not solve the problem, to perform an upgrade of the firmware. Despite this, further spontaneous failures until the end of the cruise were encountered. A more detailed description of this recently developed instrument system can be found in the report from the following cruise leg M45/3. Fig. 31 shows the results of the measurements with the LADCP on Section A and I. At the western boundary there are southwestward velocities along the Reykjanes Ridge in depths greater than 1000 m, which we expected from the southward flowing ISOW.

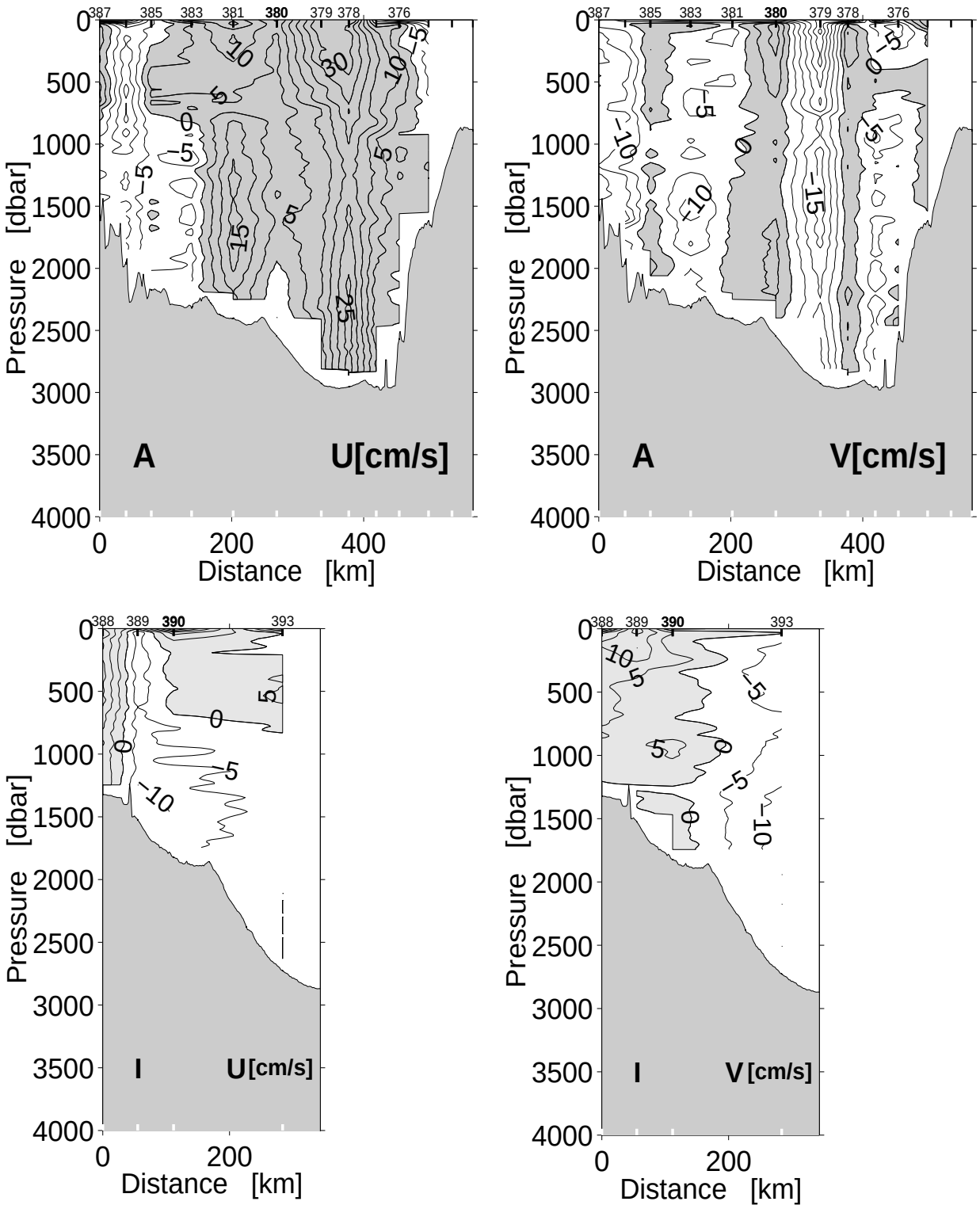

Fig. 31: Zonal (U) and meridional (V) velocities from measurements with the lowered current profiler on section A (a) and I (b).

5.2.2 Mooring Works

(T.J. Müller, D. Carlsen, P. Meyer, W. Zenk)

All mooring work is summarized in Tab. 7.2.2. Four current meter moorings that had been deployed in May 1998 as the Mid-Atlantic Ridge transport array (MART) were completely recovered. They were situated on Sec. F+G, displayed in Fig. 26. A new array with four moorings was deployed north of and in the center of Charlie Gibbs Fracture Zone. For details including acronyms see also paragraph 4, Narrative of the Cruise. One more mooring was handled: On Sec. A we exchanged mooring IM1 with our northernmost sound source for RAFOS floats. Mooring positions are labeled in Fig. 4 by bold stars with their adjacent acronyms.

All current meters of the recovered Mid-Atlantic Ridge Transport (MART) array were Aanderaa vector averaging RCM8 (Aanderaa, 1990) set to 2-hourly averaging and recording interval. All four moorings carried one instrument within the core level of the LSW, and several instruments below, the deepest one 50 m above the bottom. The following sensors showed problems:

Mooring	Depth(m)	S/N	Problem
V390/M	2780	09730	speed is zero from cycle 5500 on; rotor probably blocked
	3130	09731	direction constant at 360°
V391/A	1680	10075	speed is zero from appr. cycle 4000 to 4500
	2780	10663	speed is zero from cycle 5800 on
V393/T	2550	10076	direction from cycle 1000 on appr. Constant

As measured with pressure sensors in the uppermost instrument, vertical mooring motion did not exceed 20 m. The low pass filtered (cut off at 36 h, > 95% response at 48 h) currents somewhat surprisingly but consistently show northward flow in the deep layers at the more westerly sites M and A while strong southward and bottom intensified flow is observed at the more easterly sites R and T (Fig. 32). The reason for such a branching of the deep flow need further investigations.

5.2.3 Float works

(S. Becker, A. Pinck, W. Zenk)

Tab. 7.2.3 contains a summary of all float work. We launched eight RAFOS floats and three APEX floats on behalf of *Bundesamt für Seeschifffahrt und Hydrographie, Hamburg*. Our RAFOS floats are ballasted in two classes: 1500 m at the level of the Labrador Sea Water, and 2600 m in the Iceland Scotland Overflow Water. None of the RAFOS floats is preprogrammed to finish its mission and to return to the surface before 2001. The deployment location list also includes our float park site east of Charlie Gibbs Fracture Zone (Sta. 345). There we launched a cluster of five floats. We look forward to the exciting opportunity to compare simultaneous APEX and RAFOS drifts at the same level in the Labrador Sea Water, including the intended delayed modes of three RAFOS floats (preliminarily parked at the sea floor).

(a)

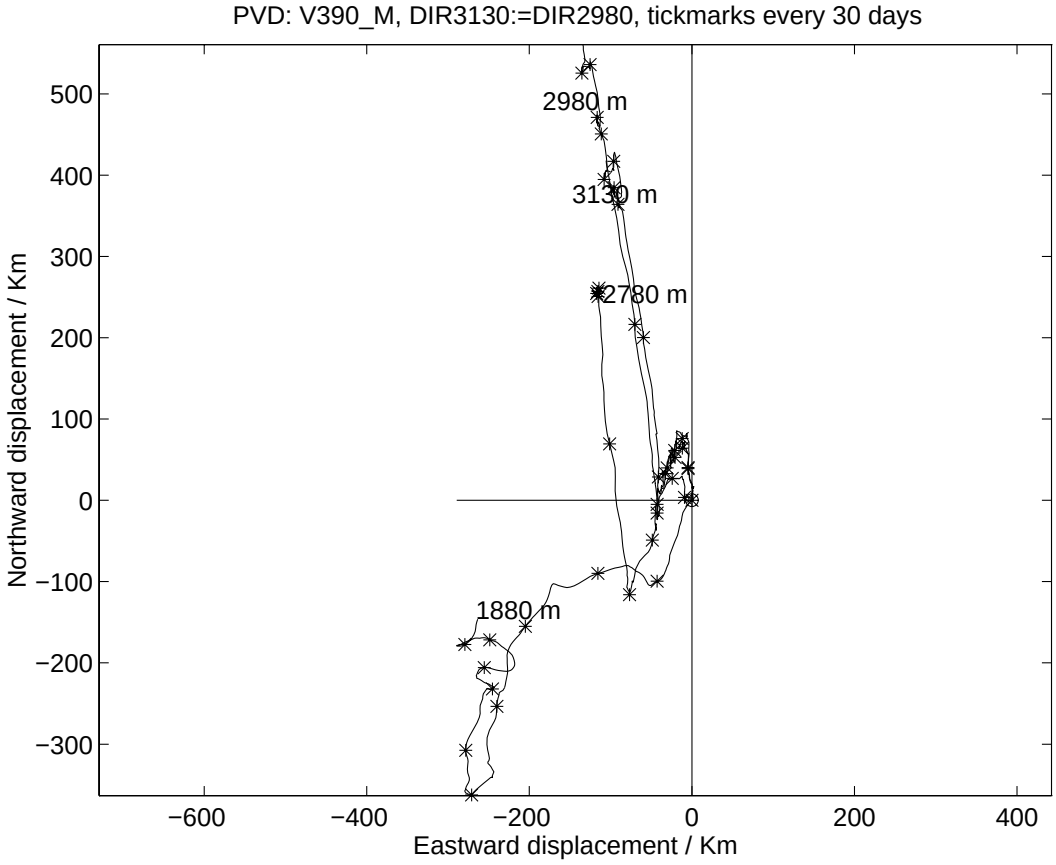

(b)

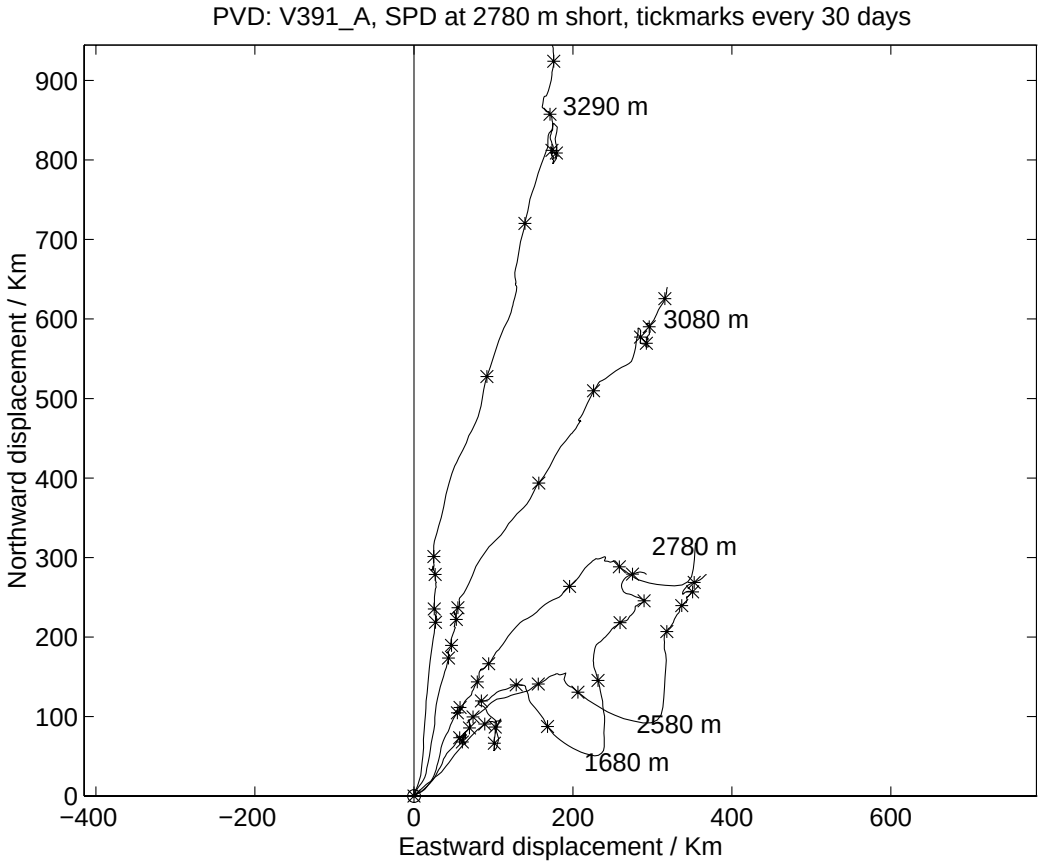

Fig. 32: Progressive vector diagrammes from low pass filtered daily averages at mooring site V390/M (a), V391/A (b), V392/R (c) and V393/T (d).

(c)

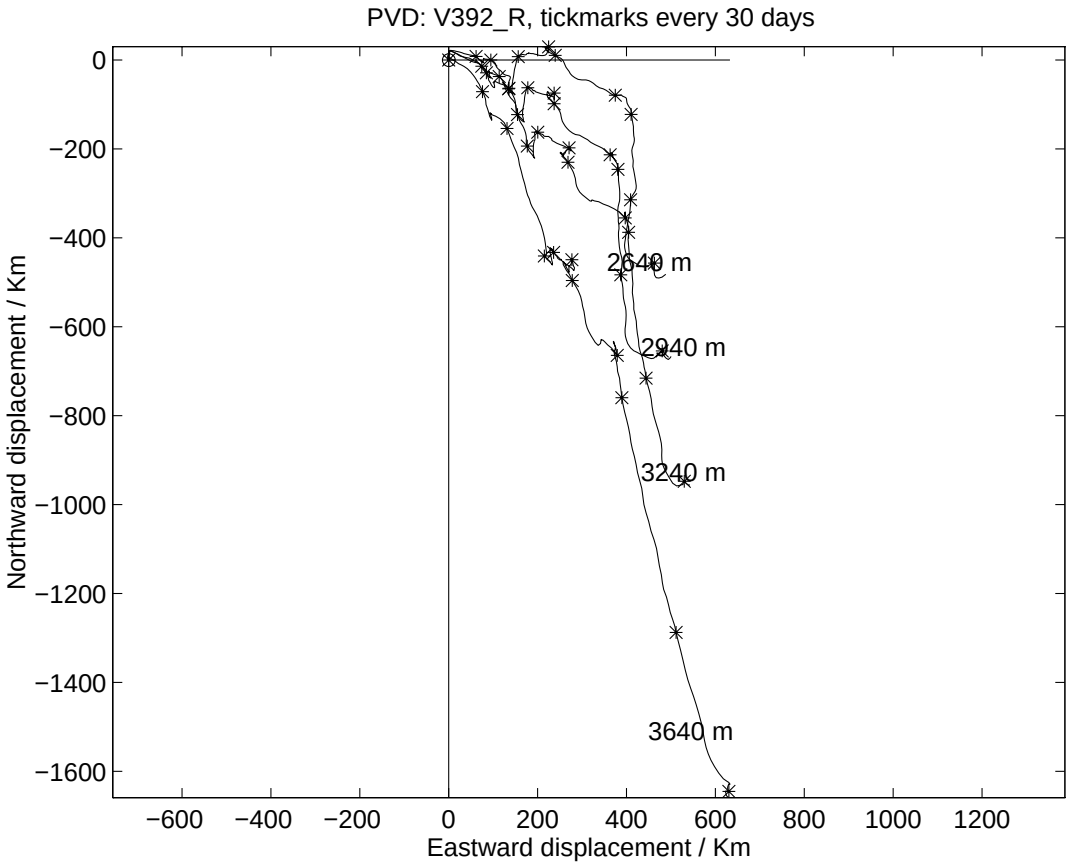

(d)

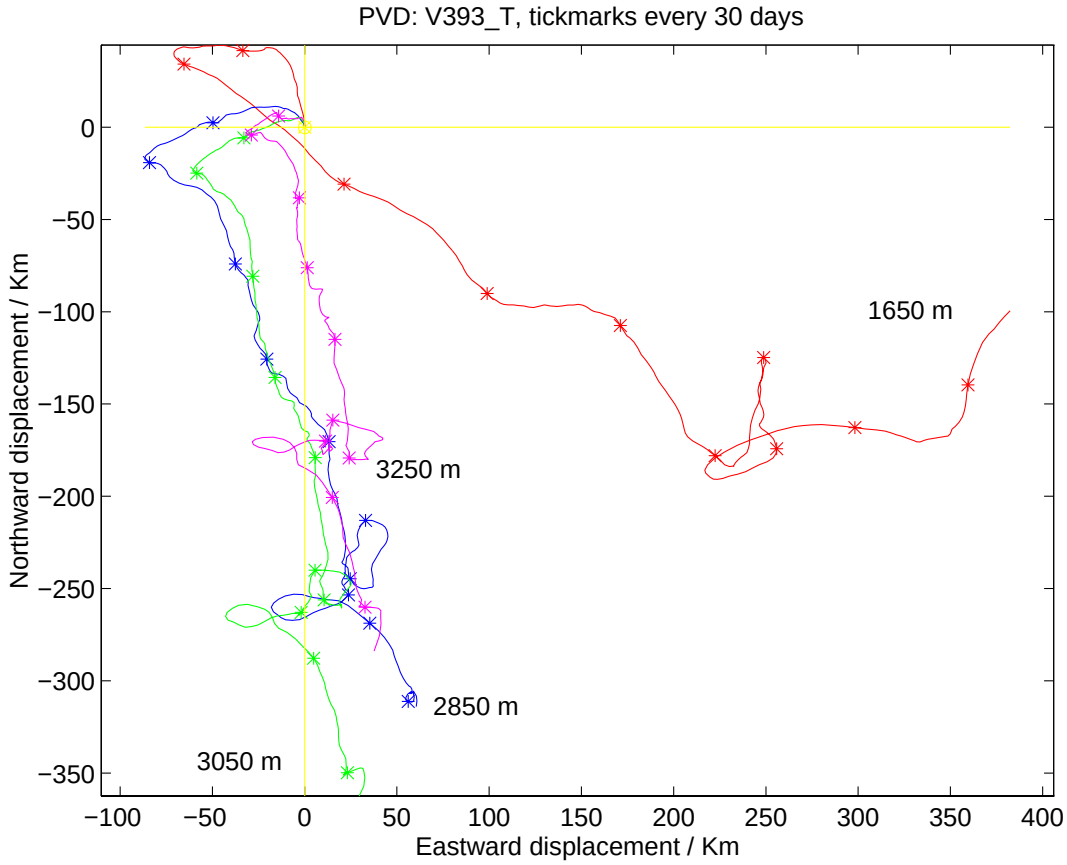

Fig. 32: continued

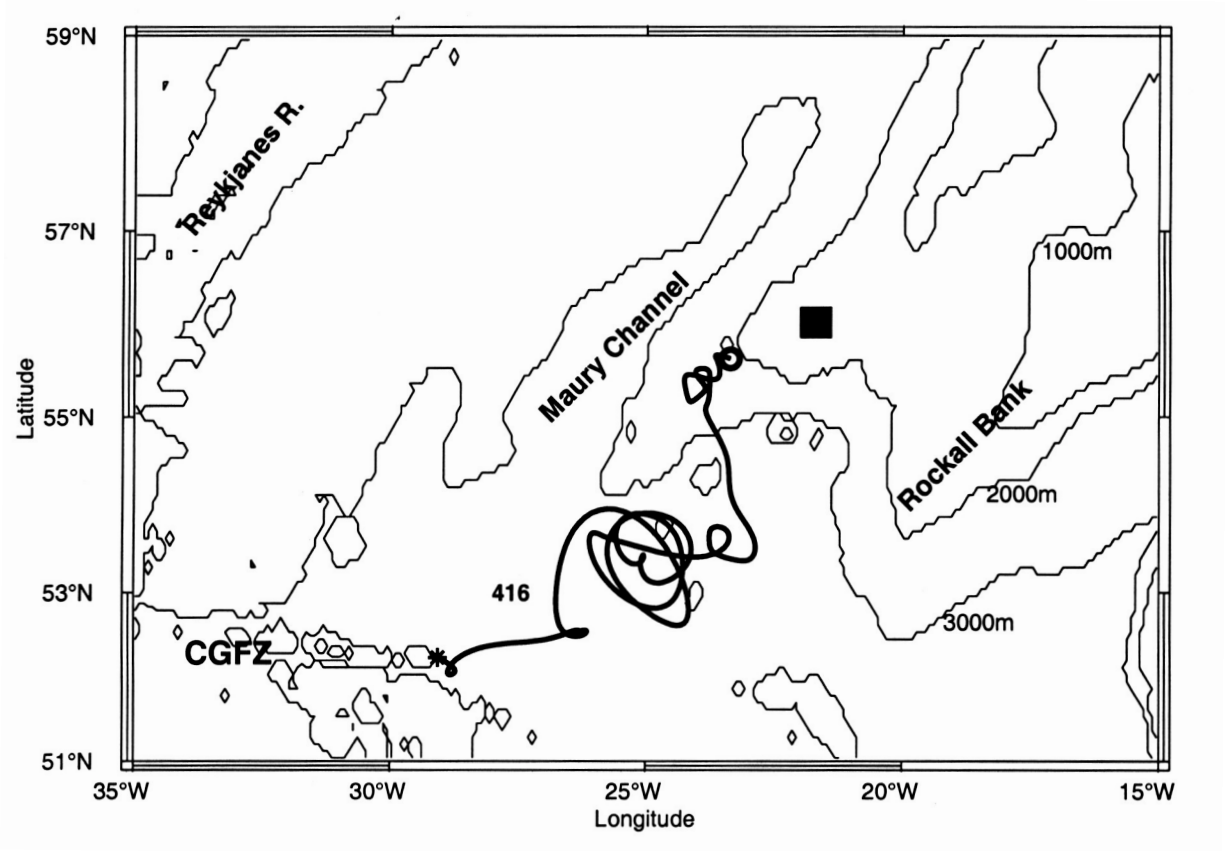

Fig. 33: Trajectory of float 416 from December 1997 - May 1999 in about 1500 m depth. The star shows the launch position, circle the surface position and square the position of recovery on Sta 372.

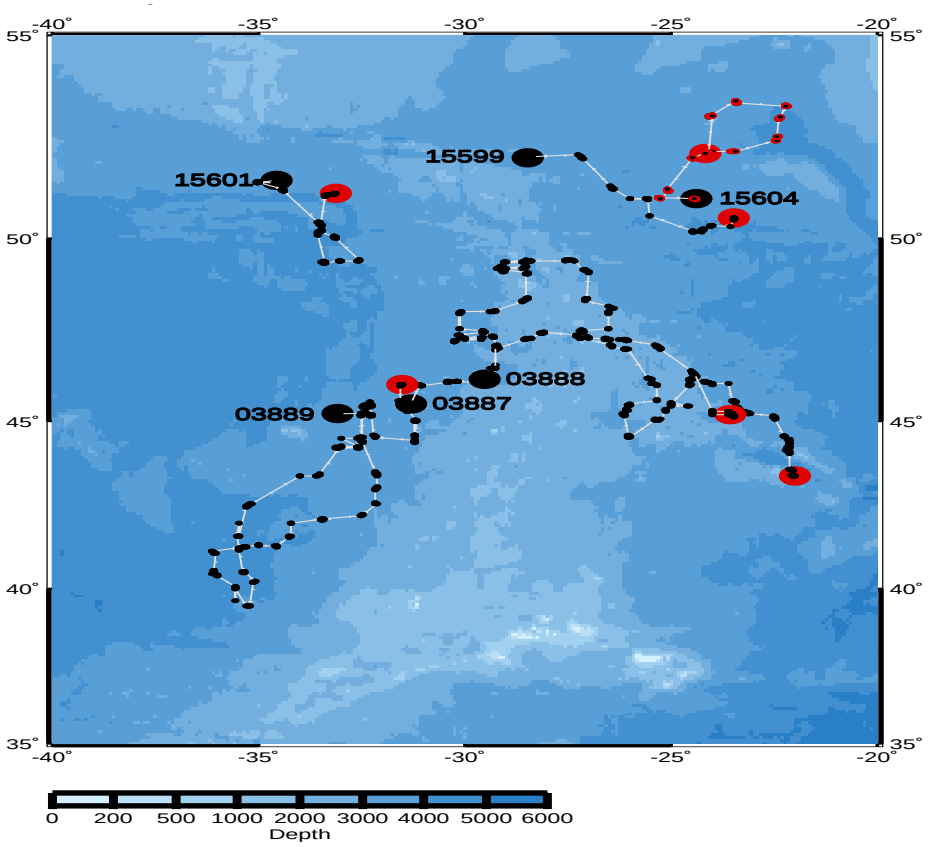

Fig. 34: Positions of profiling floats deployed across the Mid-Atlantic Ridge deployed on M45/2 (15599, 15601, 15604) and farther south one year earlier (3887, 3888, 3889) along the BSH 48°N-section. Launch positions are marked with black circles and numbers. (Status: 11/99).

RAFOS float #416 was recovered after a two year mission in the Iceland Basin. In Fig. 33 we show as an example its trajectory from December 1997 - May 1999. Float 416 is a float of our southern float park east of Charlie Gibbs Fracture Zone. It was launched in June 1997 during cruise M39/2. After a delay of 6 months it ascended to its mission level of 1500 dbar. It drifted eastward with the LSW and was entrained by an eddy in February 1998 at about 53.5°N and 26°W. In November 1998 after 8 months the float left this eddy and was advected further to the north. On 22 May 1999 its 540-day mission terminated and the float reached the surface to transmit its data.

Deployment of profiling APEX floats in the area of the Charlie-Gibbs-Fracture Zone (K.P. Koltermann)

Three APEX floats were deployed on leg M45/2 on both sides of the Charlie Gibbs Fracture Zone and right on top of it at ca. 1500 m depth. They are to surface every 14 days and relais their T/S profile data and positions back to shore. These floats complement northward a similar array maintained at the 48° N section of *Bundesamt für Seeschiffahrt und Hydrographie* (BSH) since 1996. These floats, initially deployed at the sites of long-term current-meter moorings, have stayed for a long time in an area 2° x 2°. This area is dominated by quasi-stationary eddies fixed to topographical features and are well seen in altimeter data with a 50 – 100 km diameter. Only slowly do these eddies move along the bathymetry and sometimes finally across the Mid-Atlantic Ridge.

Through annual re-seeding we have maintained a virtual time-series station that records the T/S-profile since. Similar data are otherwise not available and have proven to be of great value in assessing the winter cooling period down far below the permanent pycnocline in the area. At the same time we have been able to record the arrival of newly formed Labrador Sea Water at the site. Fig. 34 shows in the northern part at ca. 52° N the tracks of the three floats deployed now, in the southern part around 45° N the positions since the deployment one year earlier for comparison.

5.2.4 Chlorofluorocarbons

(D. Kieke, M. Rhein, J. Dankert, M. Elbrächter)

Aims

The aims of the chlorofluorocarbons (CFC) measurements are to study the deep water circulation and the variability of the tracer characteristic of the various deep water masses. Of special interest are the paths and time scales of spreading of recently formed modes of Labrador Sea Water (LSW) invading the Iceland Basin from the west.

Technical Aspects

At the begin of the cruise, the analysis of CFCs were prevented by high blanks in the purge and trap unit. After exchange of parts of the system, the blanks decreased and the first reliable measurements were carried out at Sta. 335 (CTD profile 8, see Table 7.2.1). Afterwards the system worked successfully, and about 1020 water samples were analysed. The accuracy was checked by analysing 10% of the samples twice and was found to be ±0.9% for both CFC components (CFC-11, CFC-12). Unfortunately, the closing system for the water bottles malfunctioned frequently during casts, so that the depths where the water bottles dropped were occasionally uncertain and had to be adjusted with the help of all other rosette data. Regrettably, some uncertainties remained.

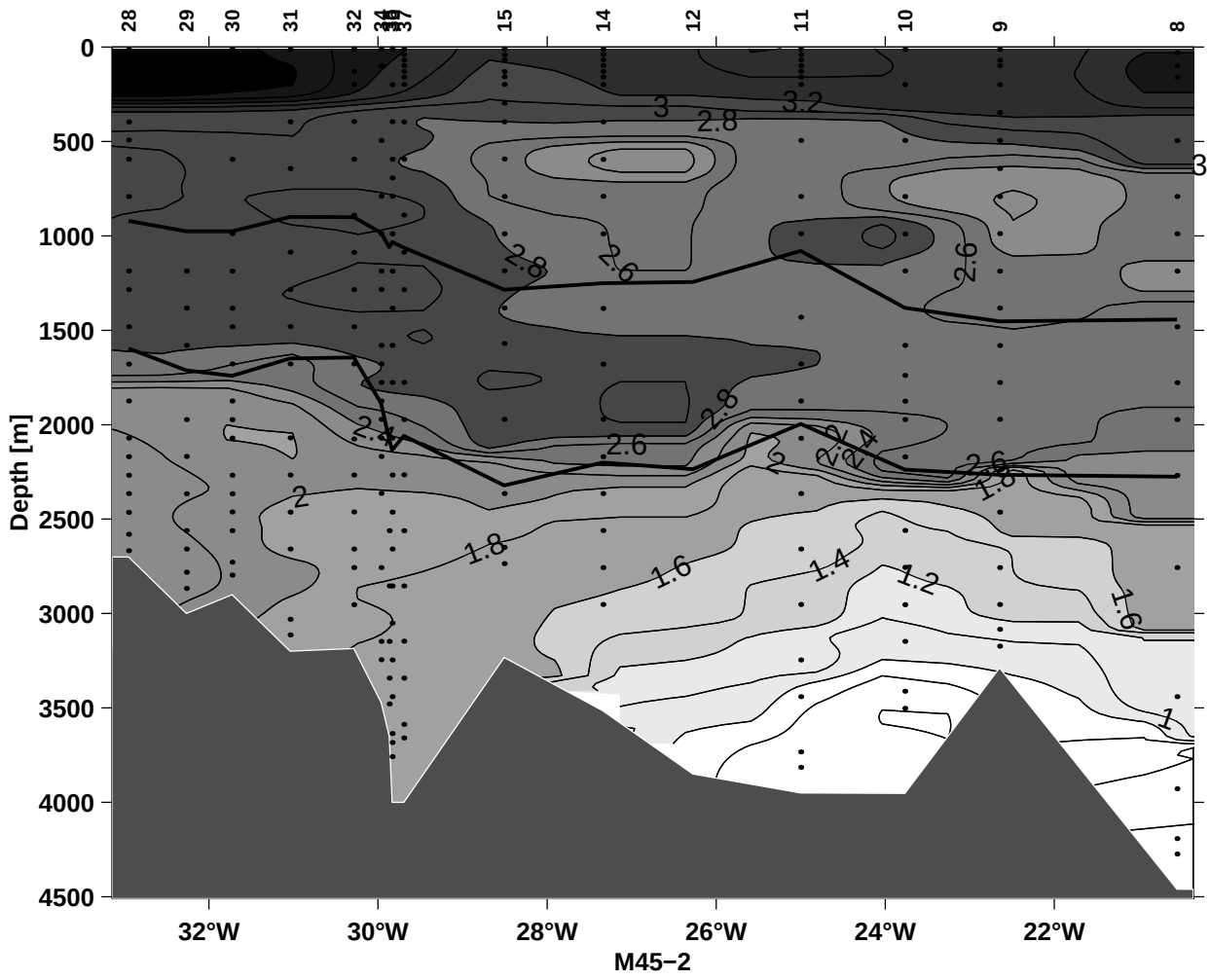

Fig. 35: CFC-11 (pmol/kg) zonal section from the Reykjanes Ridge towards the Porcupine Abyssal Plane. The thick lines are the isopycnals σ_θ = 27.74 and 27.80, which bound the LSW. The section is a composite of the profiles 8 - 15 and 28 - 37.

Preliminary results

Fig. 35 presents the CFC-11 distribution along the initial zonal section from the Reykjanes Ridge (left side) to the Porcupine Abyssal Plane (right). The CFC poor water below 3500 m east of 26° W is Northeast Atlantic Deep Water. On the flank of the Reykjanes Ridge west of 30° W and below the LSW (bounded by σ_θ = 27.74-80, thick lines in Fig. 35) the Iceland Scotland Overflow Water (ISOW) has CFC-11 concentrations of 2 - 2.3 pmol/kg on this section. On the northernmost section (CTD profiles 53 - 59, section **I**), i.e. nearer to the overflow region, the ISOW exhibits CFC-11 values greater than 3.2 pmol/kg. Further south at section **A** (CTD profiles 40 - 52), the concentrations decrease to 2.8 - 3 pmol/kg. The CFC-11 concentrations of LSW are higher on the western side of the section (>2.8 pmol/kg west of 26° W), indicating the inflow of LSW from the Irminger Sea.

Compared to 1997, the CFC concentrations in LSW still increase caused by the invasion of well ventilated, CFC rich LSW from the western Atlantic (RHEIN ET AL., 1999). Here we present the tracer distribution of lower LSW (σ_θ = 27.77 - 27.80). These density layers encompass the salinity and vorticity minimum of LSW at about σ_θ = 27.78 (Fig. 36). The flow of LSW towards the eastern side of the Iceland Basin is clearly visible in both distributions, marked with elevated CFC-11 values. Another path points further east and south into the Porcupine Abyssal Plane. High CFC-11 concentrations (>3 pmol/kg) are also found in the northernmost section (I) in 1999. This signal does not indicate a newly ventilated mode of

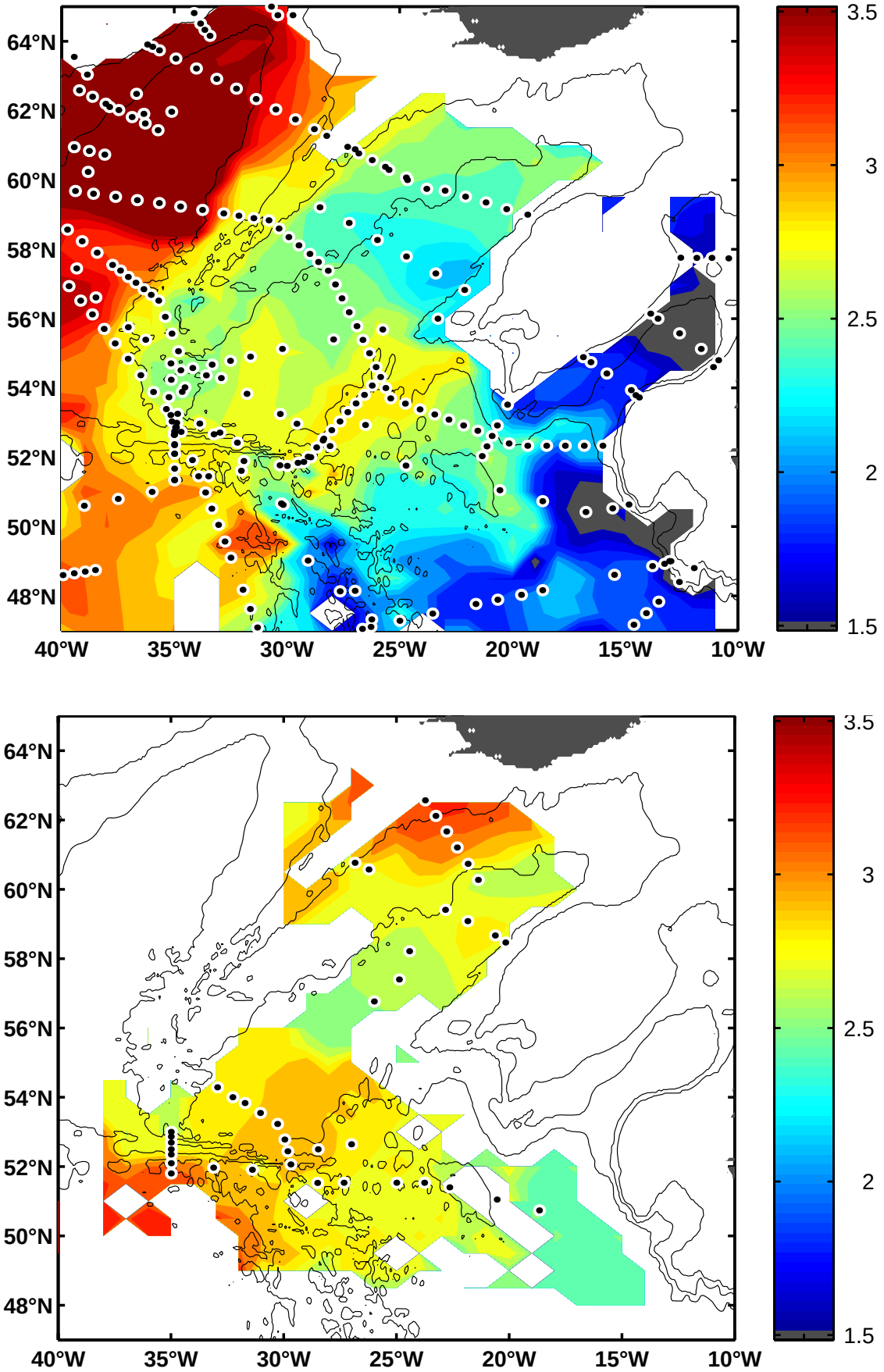

Fig. 36: Horizontal distribution of CFC-11 (pmol/kg) in Lower LSW averaged between σ_θ = 27.77 - 27.80. Top: CFC-11 distribution in 1997. Data are from M39/2 and M39/5 (SCHOTT ET AL., 1999) as well as R.V. KNORR 151 (R.WEISS, SIO, pers. comm.). Bottom: data from FS METEOR M45/2.

LSW, but the presence of the saline ISOW also at that density layer where usually LSW is found. The thickness of the σ_θ=27.77 - 27.80 at that latitude is only about 200 m, whereas at 54° N it is more like 500 - 600 m. ISOW and LSW can be separated by their different CFC-11-salinity correlation. For LSW, the CFC-11 concentrations increase with decreasing salinity, for ISOW salinity and CFC-11 run parallel (Fig. 37). On the northernmost section **I**, the water in the density layer σ_θ=27.74 - 27.80 contains mostly ISOW (black dots), further south at section **A** (+) both water masses are found, and at section **D** (*) only LSW remains in this density layer.

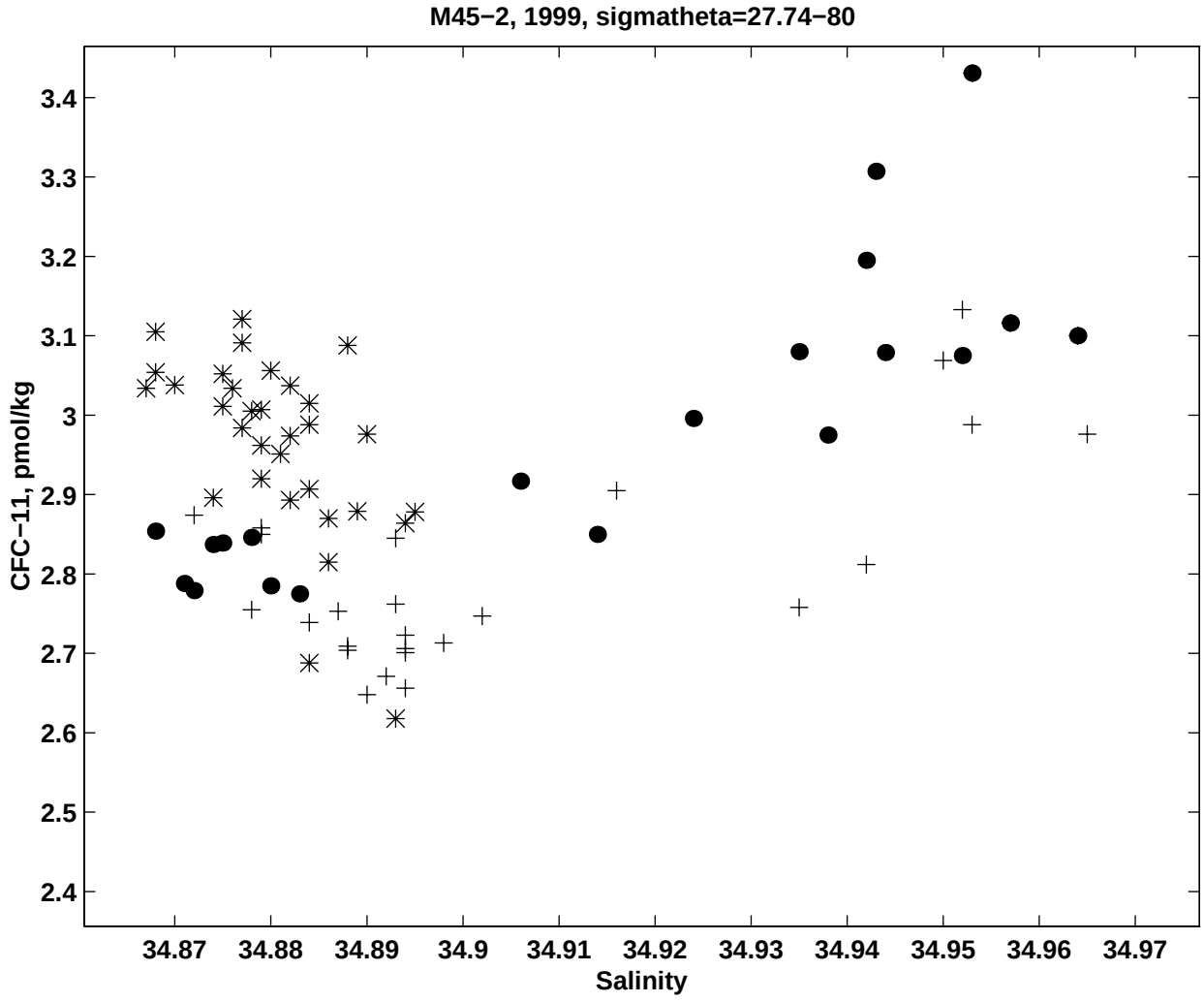

Fig. 37: CFC-11 - Salinity correlation for σ_θ = 27.74 - 27.80. Black dots: section I (CTD profiles 53 - 59), +: section A (CTD profiles 40 - 52), *: section D (CTD profiles 28 - 37).

5.2.5 Marine Chemistry

(K. M. Johnson, K. Friis, H. Johannsen, H. Frenzke)

As part of the *Sonderforschungsbereich 460* and one of its goal of documenting the uptake of anthropogenic CO_2 in the North Atlantic, we employed four independent detection strategies:

- Excess CO_2 calculation which is based on measurement of two classical marine CO_2-parameters (total dissolved carbon dioxide and pH) together with nutrients andoxygen in surface-to-deepwater profiles;
- Continuous CO_2 fugacity (fCO_2) measurements in the sea surface water;
- Determination of the carbon isotope ratio ^{12}C:^{13}C and phosphate in the water column;
- Measurement of the ^{14}C-signal in the water column in context with historical data sets.

5.2.5.1 Marine Carbon Dioxide System, Dissolved Oxygen, Nutrients

Total Dissolved Carbon Dioxide

Of the four carbonate system parameters, total dissolved carbon dioxide (DIC), alkalinity, pH, and fCO_2, the parameter for which the measurement techniques are the farthest advanced with respect to development, standarization, and experience is DIC. The completion of the WOCE Program in 1997 was the culmination of nearly 15 years of combined laboratory and successful field experience in the measurement of DIC by several groups. Hence the measurement of DIC is an integral part of the Marine Chemistry contribution to the Sonderforschungsbereich 460 and will be combined with nutrient and oxygen data to generate estimates of the anthropogenic carbon inventory in the North Atlantic. These data also form the data base against which future repeat measurements of DIC can be compared to directly measure the uptake of CO_2 for the calibration of global carbon models. In addition, the DIC results will be combined with the pH measurements made on this cruise (see below) and the appropriate thermodynamic constants to derive profiles of the other two carbonate system parameters fCO_2 and alkalinity.

Samples were collected on M45/2 in 300 mL BOD bottles. Standard techniques for dissolved gases were used for sampling (Doe, 1994). A short drawing tube extending from the Niskin bottle to the bottom of the sample bottle was used to fill the sample bottles. Care was taken to rinse the bottles in an inverted position with at least 50 mL of seawater before the bottles were turned upright and filled to at least 1 and 1/2 volumes (i.e. overflowing by at least 1/2 volume). The drawing tube was stored in seawater between use and this helped avoid bubbles during the filling operation.

For the most part, and this is an exception to the reference above (Doe, 1994), the samples were not poisoned with $HgCl_2$. The unpoisoned samples were always analyzed within 24 hours of collection. However, because a longer time between collection and analysis was anticipated for samples collected at stations 333, 348, 358, 370, and 400 these samples were poisoned with 0.05 mL of a saturated solution of $HgCl_2$. In actual fact, only for Station 400 was the analysis delayed for longer than 24 hours. A total of 548 individual water samples from 28 stations along with 50 duplicates were analyzed during M45/2 (n = 598). In addition, 36 Certified Reference Material (CRM) were analyzed.

The DIC analysis were made by SOMMA-Coulometry where SOMMA stands for Single-Operator Multiparameter Metabolic Analyzer. The SOMMA is an automated sample processor which dispenses an accurately known volume of seawater into a stripper, acidifies the seawater, removes the resultant CO_2

gas by continuous gas extraction (sparging with CO_2-free N_2 as carrier gas), dries the gas stream, and delivers the CO_2 to a Coulometer cell where it is coulometrically titrated. The sample is kept at a constant temperature of 20 °C during the analysis. Details concerning the method and the introduction, development, and calibration of the SOMMA-Coulometer System can be found in JOHNSON AND WALLACE (1992); JOHNSON ET AL. (1993); DOE (1994); GRASSHOF ET AL. (1999). The carrier gas was supplied by a Peak Model 1500 Calibration Gas Generator connected to the ship's compressed air supply otherwise all reagents remain as described by JOHNSON ET AL. (1993).

The coulometric titration is carried out in a two-chambered glass cell consisting of a rubber-stoppered main chamber (approx. 200 mL) containing a platinum or working electrode (cathode) and a secondary chamber (approx. 50 mL) in the form of an L-shaped side arm containing a pure silver electrode (anode) which is joined to the main chamber by a sintered glass frit. The main chamber is filled with a solution of DMSO containing 5 % monoethanolamine, 5 % water, an electrolyte, and a colorimetric indicator (thymolpthalein), while the secondary chamber is filled with a saturated solution of KI in DMSO and water. According to current theory (HUFFMAN, 1977), incoming CO_2 reacts quantitatively with monoethanolamine to form an acid (Hydroxyethylcarbamic acid) which is titrated by OH^- ions produced by the electrolysis of water at the cathode during the passage of electric current. The endpoint is determined photometrically by measuring the transmittance of the indicator at approximately 610 nm, and the coulometer integrates the charge (e^-) used to return the cell solution to its original color (basic = blue) after the introduction of CO_2 (acidic = colorless). Charge is related to the quantity of OH^- generated by Faraday's Constant (96485.309 C mol^{-1}), and from the amount of OH^- generated we derive the amount of acid neutralized and hence the amount of CO_2 introduced into the cell.

In well functioning systems, there is a small but measurable consistent system blank, and the computer uses this fact to recognize the end of the titration. If the computer detects that the coulometer is titrating at or below the blank level 0.005 µmol min^{-1} for 4 minutes, the computer terminates the analysis by automatically emptying the SOMMA stripper. On this basis, the typical titration time per sample ranges from 10 - 14 minutes. The software calculates DIC in µmol kg^{-1}, writes the data to a spread sheet file on the floppy disk, and displays the options menu on the computer monitor. The operator then connects the next bottle, selects the „Analyze Sample" option from the menu, inputs the sample data, including salinity, when prompted by the computer, and the process is repeated.

The system used on M45/2 (S/N032) was calibrated in three ways. First in the laboratory at the IfMK in March of 1999 by one of us (K. M. J.) before being shipped to sea for a cruise in April aboard the R/V HESPERIDES (Spain) with Dr. Ludger Mintrop who then trans-shipped it to the FS METEOR for the M45/2 cruise. The laboratory calibration was made using pure CO_2 with hardware built into the SOMMA chassis. In this procedure, two gas sample loops of differing but known volumes (to ± 0.02 %) are filled with pure CO_2 at a known temperature and pressure (temperature and pressure sensors are built into the SOMMA) and the loop contents are titrated with the calibration gas following the same route through the stripper to the coulometer as the CO_2 stripped from samples. The ratio of the calculated mass to the mass determined coulometrically is the gas calibration factor (Calfactor) used to correct the sample titrations for departures from the theoretical recovery of 100 %. Using three specific serially numbered cells, Coulometer (S/N8900-V), and SOMMA (S/N032) the mean gas calibration factor was determined to be 1.001468 (n = 5) or 99.85 %. This calibration factor was entered into the software and used to calculate sample DIC in µmol kg^{-1} according to the relationship:

$$DIC = Calfactor * \mu mol * (1000 / V_T * \rho)$$

where Calfactor is the gas calibration factor, µmol is the result of the sample coulometric titration, V_T the sample volume at the sample temperature (T = 20°C), and ρ the density of sea water at the sample temperature and salinity. The same three laboratory calibrated cells were used throughout the two cruises. Aboard ship the system was calibrated by analyzing Certified Reference Material (CRM) bottles which contain seawater with a known or certified DIC concentration. The CRM were prepared by Dr. Andrew Dickson and analyzed by Dr. C. D. Keeling by vacuum extraction with manometric detection at the Scripps Institution of Oceanography in La Jolla, CA. Lastly, gravimetric determinations of the sample volume (V_T) at 20 °C were made before the cruise and in St. John's at the completion of the cruise. System Performance is given in Table 5.

Table 5: Accuracy and Precision of SOMMA-Coulometer system 032 during the M45/2 Cruise. Part I: Accuracy based the analysis of the CRM. Part II: Precision from the duplicates collected for 50 of the 548 Niskin bottles sampled. Sample precision is given as the mean absolute difference between duplicates. The duplicates were either analyzed on the same day collected (with the same coulometer cell) or on a different day usually the day after collection with a different cell. Standard deviations are indicated by the ± symbol.

Part I. Accuracy (Analysis of the CRM)

Analyzed	Mean DIC s. d. (µmol kg^{-1})	Certified DIC (µmol kg^{-1})	Mean Diff. (µmol kg^{-1})
36	1993.85 ± 1.55	1994.17 ± 0.93	- 0.32

Part II. Precision (CRM and 50 sample duplicate pairs)

CRM	All Duplicates (n) mean (µmol kg^{-1})	Same Day (n) mean (µmol kg^{-1})	Different Day (n) mean (µmol kg^{-1})
1.55	0.80 (50) ± 0.64	0.64 (35) ± 0.51	1.17 (15) ± 0.77

A preliminary plot of DIC vs. depth from stations 330 to 334 is shown in Fig. 38 (top). These data illustrate the three typically representative DIC groups found in the surface, intermediate, and deep waters, respectively. In addition, within these groups water masses with differing origins and ages can be seen. The high deep water DIC, between 2185 and 2205 µmol / kg, are representative of the older AABW, while the „outbreak profile" observed at station 330 with even higher DIC between 1500 and 4000 dbar has its origin in the Intermediate Mediterranean Water (IMW). The deep water DIC data also shows evidence of a third but as yet unidentified water mass.

Spectrophotometric pH_T Determination

In addition to DIC, pH (on the total scale = pH_T) was measured on the same samples. A total of 659 samples were analyzed (n = 588). The samples were taken in 500 mL bottles in the same way and with the same precautions as for DIC (see above). The measurements were made using meta-cresol purple as indicator dye with a new automated spectrophotometric system based on Friis (1997). The analyzer hardware conformed to specifications given in Doe (1994). The indicator dye was dissolved in seawater and for analysis the mixing ratio (sample:indicator) was 660:1. Four samples were analyzed per hour on this system, and all raw data were stored separately to facilitate post-cruise corrections when final cruise salinities are available. The precision of the pH determination was determined by analyzing the CRM used for DIC (see above) on a daily basis, and for these analysis the precision was ± 0.0015 pH units (n = 20).

The pH_T vs. depth profiles from stations 330 to 394 are compiled and given in Fig. 38 (middle). The pH plot is virtually the mirror image of the DIC. Due to biological processes pH_T is highly variable in the surface waters and ranged from a high of 8.070 to a low of 7.930, but it becomes most acidic in the younger intermediate water masses due to the uptake of CO_2 from the atmosphere while these waters were at the surface and due to respiration as they sink. With greater depth the pH signature is more homogenous and acidic.

The pH_T vs. DIC plot given in Fig. 38 (bottom) shows in general a strong negative correlation over the DIC and pH_T dynamic ranges. The correlation is weakest in the surface waters where biological activity and gas exchange (wave action) is highest, increases in the intermediate waters where respiration is predominant, and at DIC concentrations exceeding 2180 µmol kg-SW^{-1} the pH_T does not change. The latter is again characteristic of the AABW where the higher DIC in this old water mass is brought about by particle remineralisation and calcium carbonate dissolution beyond the aragonite and calcite lysocline.

Nutrients and Oxygen

Nutrients (nitrate, nitrite, phosphate, silicate) and oxygen were determined from every Niskin bottle. The nutrient analysis was made with an autoanalyzing system according to GRASHOFF ET AL. (1999). The accuracy for nutrient analysis was 1 % of the nutrient standards. This is 0.205 µmol kg-SW^{-1} for nitrate, is 0.005 µmol kg-SW^{-1} for nitrite, is 0.025 µmol kg-SW^{-1} for phosphate and 0.5 µmol kg-SW^{-1} for silicate. For oxygen determination a standard titration after Winkler (GRASHOFF ET AL., 1999) was used.

5.2.5.2 Sea Surface fCO_2

The second analytical strategy involved the continuous determination of the fugacity of CO_2 in surface water and in the overlying atmosphere. For this purpose an automated underway fCO_2 system (KÖRTZINGER ET AL., 1996) with a non-dispersive infrared gas detector for CO_2 was continually operated along the cruise track. A continous flow of seawater was drawn at 5 m depth from the ship's "moon pool" which was equipped with a CTD. Every 2 minutes a fCO_2 data point together with temperature and salinity from the CTD were logged along with the position data from an independent GPS system. Previous work (KÖRTZINGER ET AL., 1996) has shown that the system is accurate and precise to ± 2 µatm.

The preliminary fCO_2 shipboard results (Fig. 39) illustrate typical aspects of fCO_2 in the central North Atlantic during the summer months:

- CO_2 sea surface conditions with fCO_2 undersaturation up to differences from 100 µatm are not rare.
- Plankton blooms and high photosynthesis activity are clearly seen in a decrease of sea surface fCO_2.
- Sea surface temperature increase should lead to (from the thermodynamic point of view) an increase in fCO_2, but this effect is masked by the biological processes.
- Sea surface temperature decrease should lead to a fCO_2 decrease through increased gas solubility, but this maybe compensated for by a net CO_2 flux from the atmosphere into the ocean.

5.2.5.3 Carbon Isotope ^{13}C

The third method to estimate the net CO_2 ocean uptake in the North Atlantic is based on the Suess-effect. The Suess-effect depends on changing ^{12}C to ^{13}C ratios in the atmosphere due to fossil fuel combustion. A relatively homogenous ^{12}C to ^{13}C ratio in the atmosphere has a strong counterpart in the ocean. This is

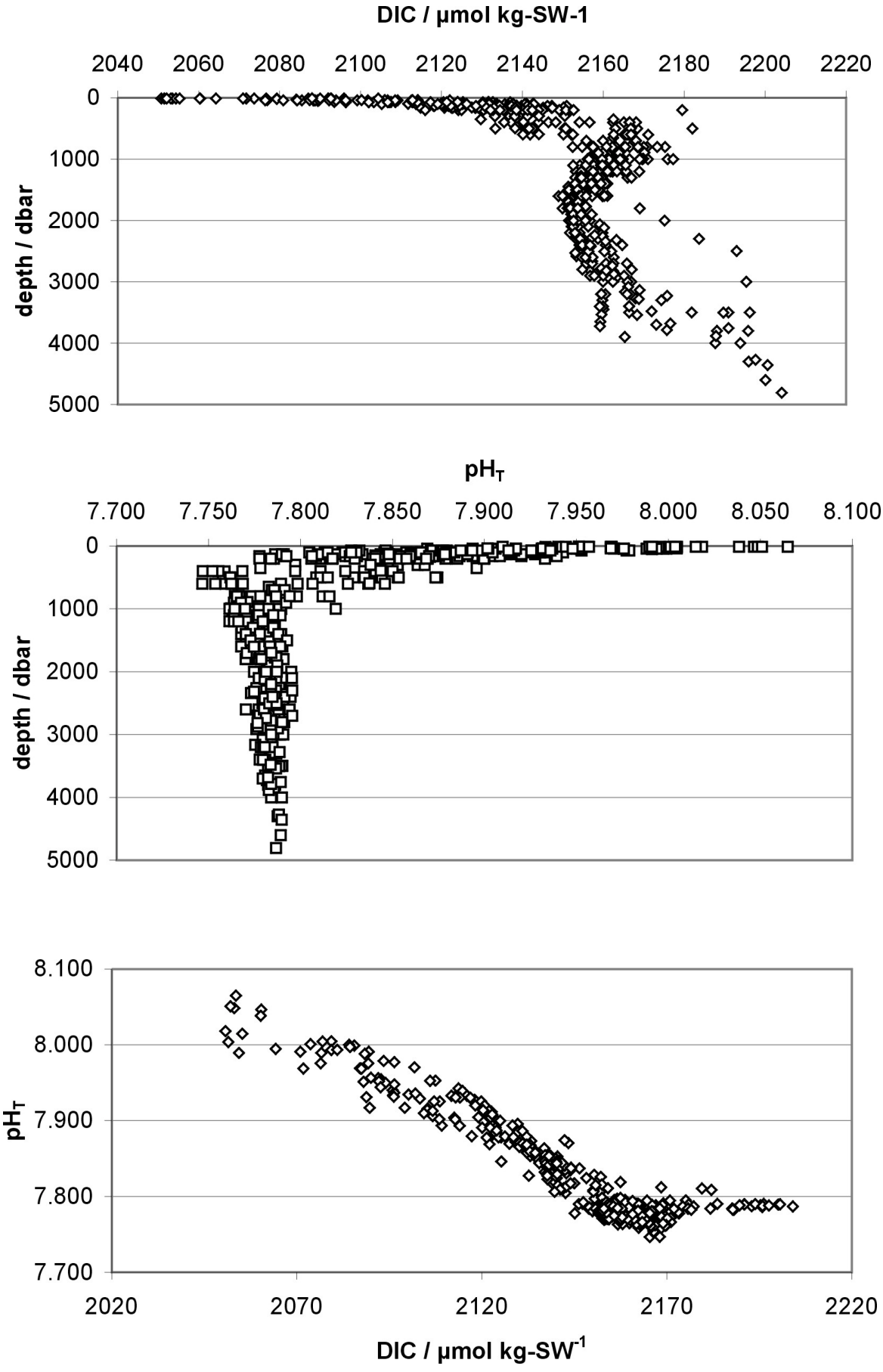

Fig. 38: DIC and pH_T (T = 22 °C) plots for the stations 330 - 394.

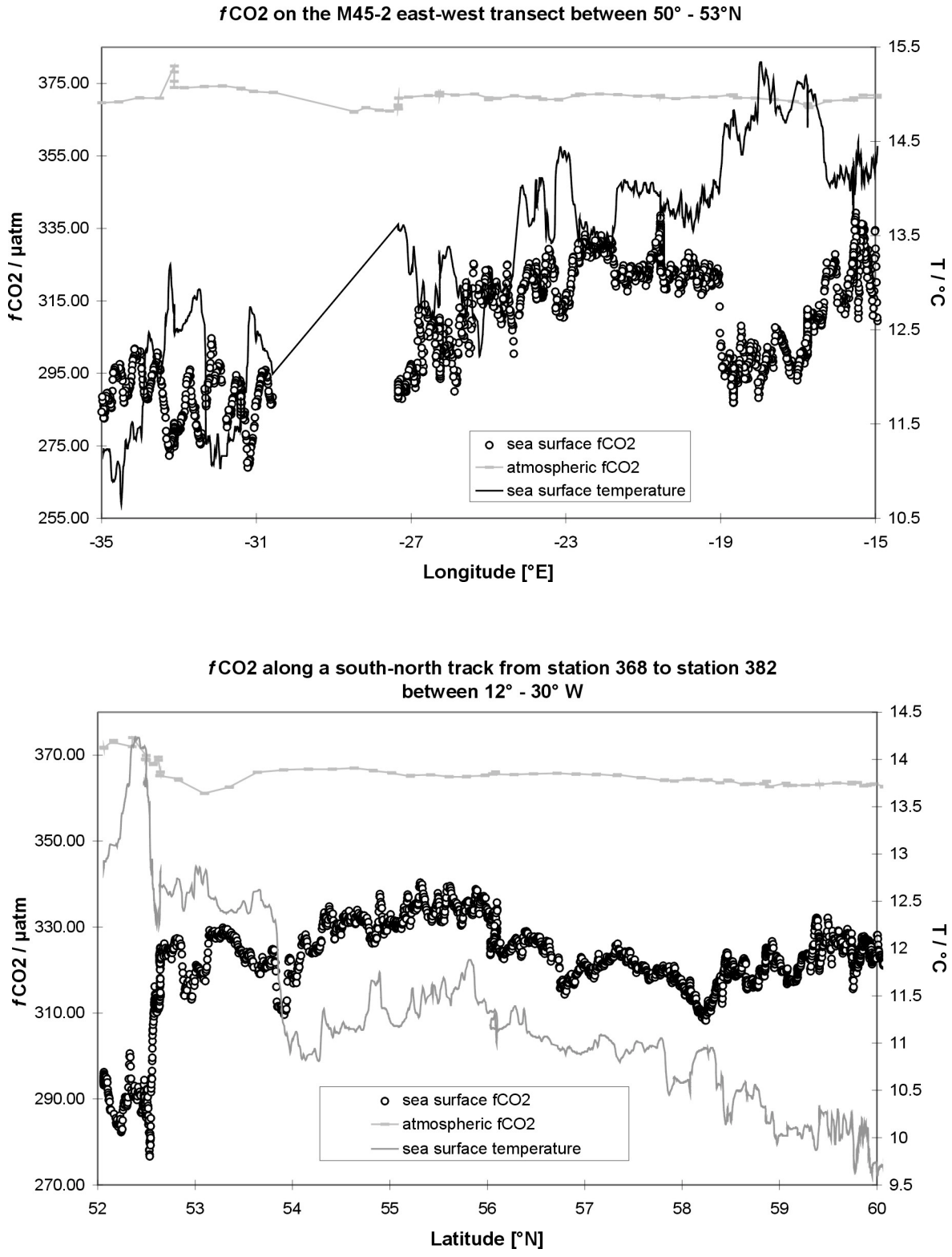

Fig. 39: Fugacity of CO_2 on two different transects on M45/2

because of longer isotopic equilibrium timescales in the surface ocean and much slower mixing ratios in the ocean than in the atmosphere. Measurements of the disequilibrium in isotopic ratios (together with phosphate measurements) can provide an estimate of CO_2 uptake.

On leg M45/2, 567 samples for ^{13}C mass spectrometer analysis were collected. Each 100 mL bottle was carefully taken, poisoned with 50 µL $HgCl_2$ and afterwards crimp-sealed for storage and later analysis onshore.

5.2.5.4 Carbon Isotope ^{14}C

The forth and last method for CO_2 uptake documentation in the North Atlantic is based on "bomb" ^{14}C. In the late fifties and early sixties there was a strong increase in atmospheric ^{14}C concentration due to atmospheric atomic weapon testing. This strong unnatural ^{14}C peak in the atmosphere caused a strong ^{14}C disequilibrium between atmosphere and ocean and therefore an input into the ocean. Although the ^{14}C data set is very incomplete there are historical data on key positions in the North Atlantic from GEOSECS (1972 -1973), TTO (1981) and further Meteor cruises M18 and M30. The continuation of the ^{14}C time series on different key positions in the North Atlantic will be a powerful tool to verify global carbon models.

On M45/2 six historical ^{14}C (also ^{13}C) hydrocast locations were repeated as shown in Table 6.

Table 6: M45-locations at or near to historical (previousley sampled) stations with number of ^{14}C samples collected.

M45/2		GEOSECS		TTO	
Station	Number	Station	Number	Station	Number
330	21			115	13
333	20			117	12
370	18			121	17
394	20	23	18		
398	19			130 / 132	23
400	22	3	17	214	19

5.2.6 Tracer / Helium/ Tritium

(C. Wild, U. Fleischmann)

During Leg M45/2 189 samples have been taken for helium, and 179 samples for tritium measurements (Fig. 40). Approximately 42 ml of water are filled into copper tubes for the helium measurements. They had to be rinsed thoroughly and banged along the side to ensure that no air is included in the sample. The gas will be extracted from the samples and measured masspectrometically in the laboratory at the Universität Bremen.

One litre of water is filled into a glass bottle for the tritium measurements. All gas will be extracted from the water in the laboratory. Afterwards the water will be stored. During the storage time Tritium decays to ^{3}Helium, which also is measured masspectrometrically.

The main focus of the measurements during M45/2 was on the cold water sphere including the LSW core. The observations are intended for a better understanding of the formation processes of the North Atlantic Deep Water in the eastern North Atlantic. Additionally, surface samples were taken to continue the input function for Tritium in the North Atlantic and to get information on the helium saturation in surface waters.

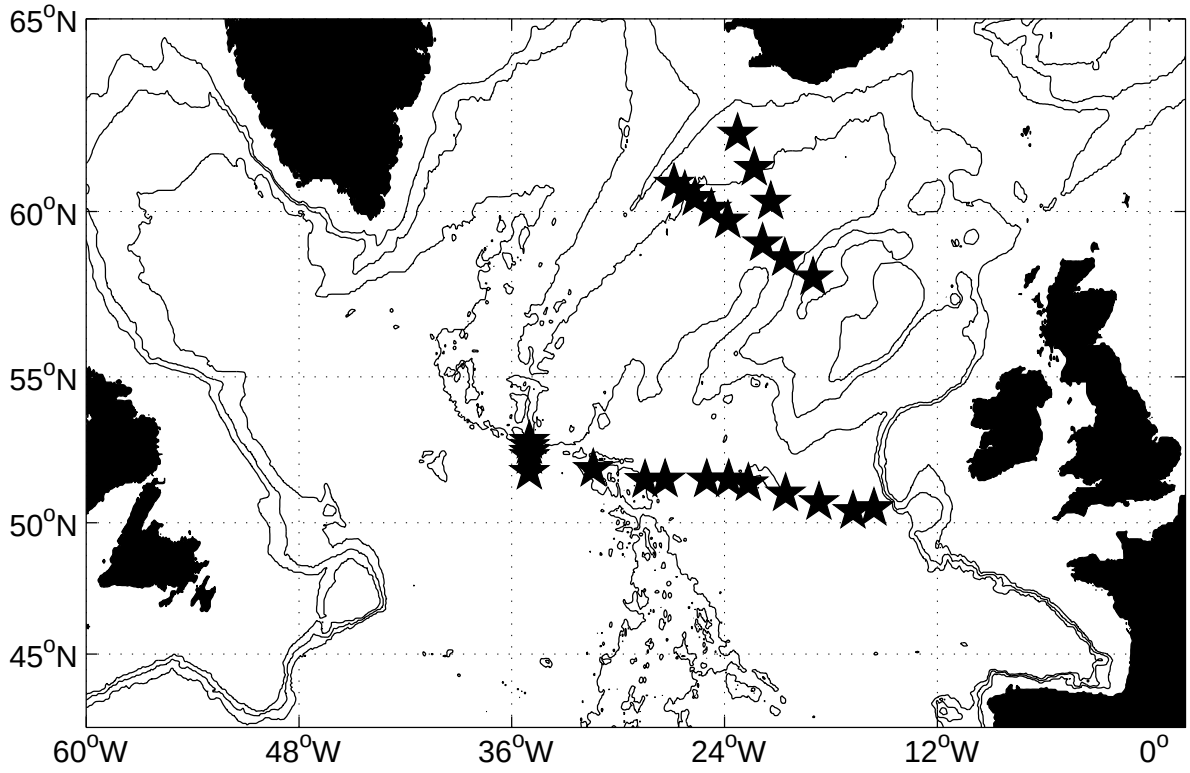

Fig. 40: 26 positions where helium- and tritium samples were taken from.

5.2.7 Natural Radionuclides

(J. Fitzke, J. Scholten)

Natural radionuclides (e.g. ^{231}Pa, ^{230}Th) are important tracers in studying the path ways of ocean particles from the water column to the sediments. Because of their particle reactivity their distribution in the water column is believed to be closely linked to the vertical particle flux. A recent investigation in the eastern North Atlantic indicated, however, that lateral advection of newly formed water masses (Labrador Sea Water, Iceland-Scotland Overflow Water) may significantly influence the radionuclide concentration-depth profiles (VOGLER ET AL., 1998).

In order to study in more detail the effects of the eastern North Atlantic hydrography on the distribution of ^{230}Th, ^{231}Pa, and Nd-isotopes, water samples were collected from seven locations in the eastern North Atlantic (Fig. 41). Water samples in the area of the Charlie Gibb Fracture Zone were obtained in order to study the effect of water mass exchange between the eastern and western North Atlantic basins as well as to investigate possible influences of the Mid-Atlantic Ridge hydrothermal activity on the tracer concentrations. The water samples obtained from the Iceland basin will allow to determine the tracer distribution in the Iceland-Scotland Overflow Water and Labrador Sea Water. The water-column profile sampled near the western European shelf will provide information about the effects of boundary scavenging at the European continental margin on the tracer distribution.

Water samples (10l) were filled in plastic containers, acidified and transported to the home labs for further isotope analyses. One litre will be taken for ^{230}Th determination by means of High-Resolution-ICP-MS, the remaining sample will be analysed for ^{231}Pa and Nd-isotopes using Thermal-Ionization Masspectrometry.

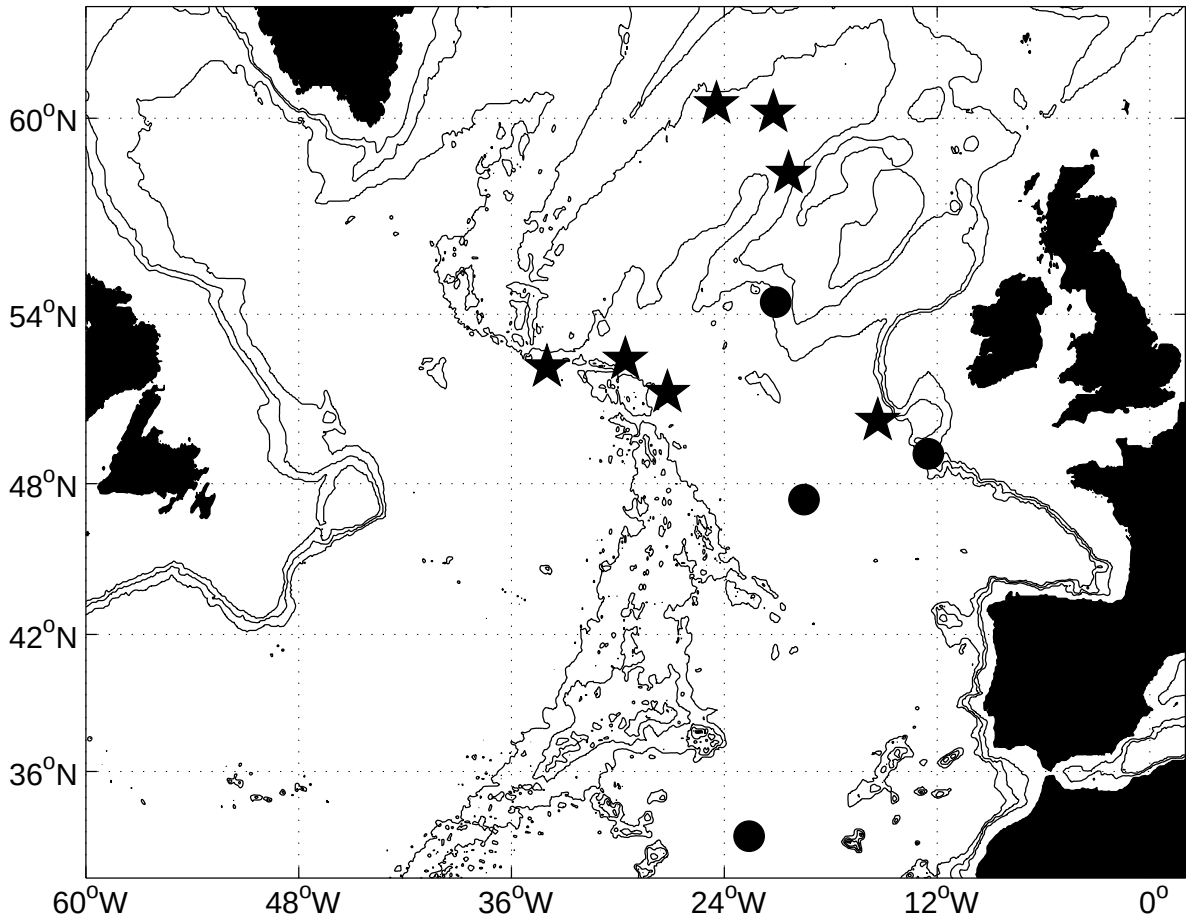

Fig. 41: Locations of water profiles collected during M45/2 (★) and JGOFS and OMEX sediment trap locations (●).